Table 1 Relationship between clinicopathological characteristics and histological necrosis

Characteristics	No. of patients	Necrosis: Presence	Necrosis: Absence	P
Age, years				
<60	123	75	48	
⩾60	225	148	77	0.414
Sex				
Male	206	143	63	
Female	142	80	62	**0.017**
Localisation				
Pancreas head	228	147	81	
Pancreas body or tail	109	70	39	1.000
Size (mm)				
<30	83	42	41	
⩾30	265	181	84	**0.004**
Pathologic tumour status				
T1	6	1	5	
T2	3	3	0	
T3	339	219	120	
T4	0	0	0	**0.023**[a]
Pathologic node status				
N0	64	33	31	
N1	284	190	94	**0.030**
Pathologic metastasis status				
M0	310	193	117	
M1	38	30	8	**0.049**
Stage				
IA	3	0	3	
IB	2	2	0	
IIA	59	31	28	
IIB	246	160	86	
III	0	0	0	
IV	38	30	8	**0.009**[a]
Tumour histological grade[b]				
W/D	90	41	49	
M/D	181	122	59	
P/D	77	60	17	**<0.0001**[a]
Tumour margin status				
Negative	249	166	82	
Positive	100	57	43	0.085
Nerve plexus invasion[b]				
Absence	112	65	47	
Presence	236	158	78	0.120
Lymphatic invasion[b]				
0, 1	102	58	44	
2, 3	246	165	81	0.086
Venous invasion[b]				
0, 1	124	63	61	
2, 3	224	160	64	**0.0002**
Intrapancreatic neural invasion[b]				
0, 1	141	86	55	
2, 3	207	137	70	0.363
Recurrent site[c]				
Local	54	39	15	
Distant sites	198	134	64	0.620
Expression of CAIX in cancer cells[d]				
Absence	114	69	45	
Presence	89	63	26	0.143
Expression of CAIX in stromal cells[d]				
Absence	74	31	43	
Presence	129	101	28	**<0.0001**
Total	348	223	125	

Abbreviations: CAIX = carbonic anhydrase IX; M/D = moderately differentiated adenocarcinoma; P/D = poorly differentaited adenocarcinoma; W/D = well-differentiated adenocarcinoma. [a]Comparisons of qualitative variables are performed using the χ^2 test, and otherwise by Fisher's exact test. [b]Classified according to the classification of pancreatic carcinoma of Japan Pancreas Society. [c]Number of patients with tumour recurrence was 252. [d]Number of patients used in the immunohistochemical analysis was 203. Statistically significant in bold values.

gastrointestinal tract pathology. These observers were provided with the definition of 'histological necrosis' according to Figure 1 and with the definitions for lymphatic, venous, and neural invasion stated in the classification of JPS (Japan Pancreas Society, 2003). They were asked to assess the presence of histological necrosis and each of the grades of lymphatic, venous, and neural invasion evident within each of the provided slides. These observers were blind to the identity of the original reviewers or those of each other. They were also not provided with any clinical information on the outcome of the patients.

Immunohistochemical analysis

Immunohistochemistry was performed on formalin-fixed, paraffin-embedded tissue sections as described previously (Takahashi *et al*, 2007), using antibodies against CAIX (M75, 1:200) (Pastorekova *et al*, 1992; Zavada *et al*, 2000) and HIF-1α (54, 1:500, BD Transduction Laboratories, Franklin Lakes, NJ, USA). Avidin–biotin complex method and CSA system (DAKO, Glostrup, Denmark) were used for these immunohistochemistry, respectively. The sections were autoclaved in the buffer (pH 9.0, Nichirei Biosciences, Tokyo, Japan) for antigen retrieval. For immunohistochemical examination of CAIX in PDCs, we used sections of representative blocks from 203 cases of PDC. Carbonic anhydrase IX is expressed always in the crypt enterocytes of the duodenum and sometimes in normal epithelial cells of the pancreatic duct and pancreatic intraepithelial neoplasm. These cells were used as the positive control for CAIX immunohistochemistry. Immunohistochemistry was performed without primary antibody for negative control. When more than 20% of cancer cells in the specimen expressed CAIX, the case was judged as positive for CAIX in cancer cells. When there were any stromal cells expressing CAIX in cancer tissue, the case was judged as presence of stromal cells expressing CAIX.

Statistical analysis

Comparisons of qualitative variables were performed using the χ^2 test or Fisher's exact test. One-way analysis of variance was used to compare the means of three or more groups. The postoperative disease-free survival (DFS) and disease-specific survival (DSS) rates were calculated by the Kaplan–Meier method. Univariate analysis was performed for prognostic factors using the log-rank test. The factors found to be predictive by univariate analysis were subjected to multivariate analysis using the Cox proportional hazards model (backward elimination method). Interobserver

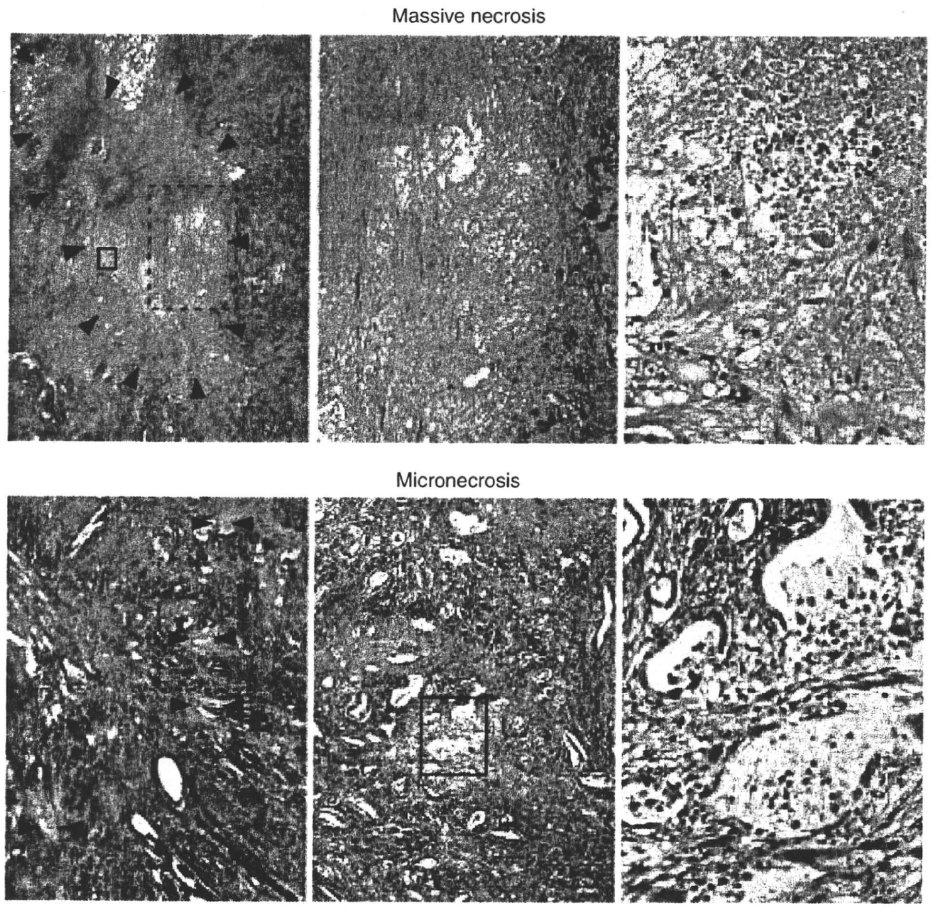

Figure 1 Representative histology of massive necrosis (upper columns) and micronecrosis (lower columns). Arrows indicate necrotic area. Left, centre, and right columns are in low (× 6.25), middle (× 20), and high magnification (× 100), respectively. High power view of histology in right columns corresponds to the rectangle (solid line) in left or middle column. Middle power view of histology in centre columns corresponds to the rectangle (dotted line) in left columns.

agreement (reproducibility) was tested by obtaining the κ-scores (Fleiss, 1971; Landis and Koch, 1977). Differences at $P<0.05$ were considered statistically significant. Statistical analyses were performed with StatView-J 5.0 software (Abacus Concepts, Berkeley, CA, USA).

RESULTS

Correspondence of both massive necrosis and micronecrosis with hypoxic foci

Immunohistochemical analysis revealed that CAIX was expressed in cancer cells or stromal cells within or around areas of both massive necrosis and micronecrosis (Figure 2).

Prognostic significance of the presence of hypoxic foci detected by expression of CAIX in cancer stromal cells

Survival analysis showed that the presence of hypoxic foci with expression of CAIX in stromal cells in cancer tissue was closely associated with shorter DFS ($P=0.004$) and DSS ($P=0.003$) (Figure 3). The presence of cancer cells expressing CAIX was also associated with shorter survival rates (Figure 3), although its occasional expression in cancer cells forming well-differentiated glands distant from necrotic areas probably indicated a cellular phenotype similar to that of normal ductal epithelial cells, and was unrelated to hypoxia. Then we used expression of CAIX in cancer stromal cells as hypoxic marker in this study. Multivariate Cox regression analysis revealed that the presence of hypoxic foci was an independent predictor of shorter DFS ($P=0.005$) and DSS ($P=0.011$) (Supplementary Table 1). The presence of necrosis was significantly correlated with the presence of hypoxic foci (Table 1). More CAIX-expressing cells were found in larger areas of necrosis.

Histopathological evaluation of PDC

Table 1 lists the clinicopathological features of patients with PDC. When correlations with these clinicopathological features were analyzed, the presence of necrosis was found to be more likely in cases with large tumours ($P=0.004$), higher tumour status ($P=0.023$), presence of nodal metastasis ($P=0.030$), presence of distant metastasis ($P=0.049$), higher TNM stage ($P=0.009$), poorer tumour differentiation ($P<0.0001$), and more frequent venous invasion ($P=0.0002$).

Prognostic significance of the histopathological valuables

Survival analysis demonstrated an association between the presence of necrosis and shorter DFS ($P<0.0001$; HR = 2.007; 95% CI: 1.531 - 2.630) and DSS ($P<0.0001$; HR = 2.196; 95% CI:

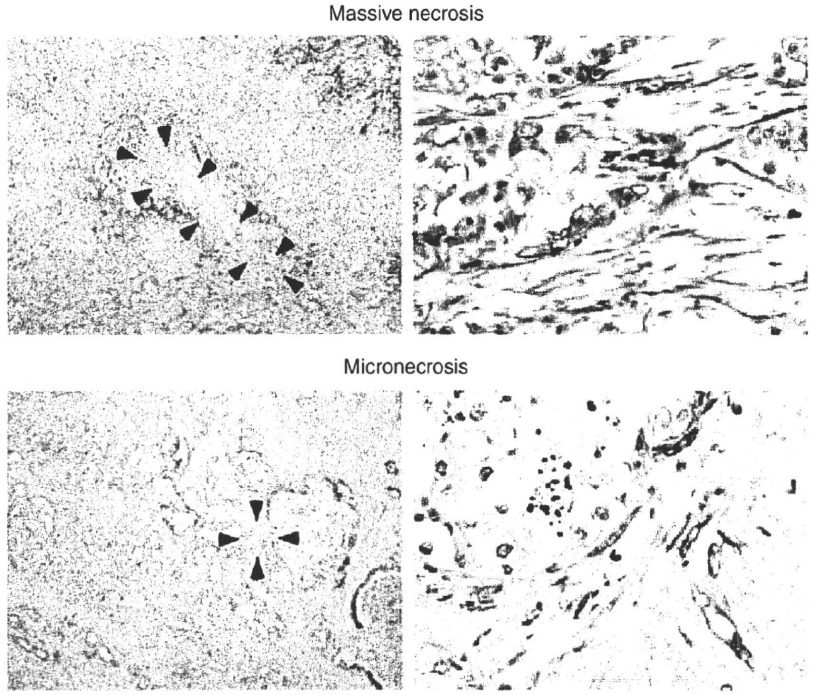

Figure 2 Hypoxia is reflected by the presence of massive necrosis or micronecrosis. Expression of CAIX is immunohistochemically detectable in both cancer cells and stromal cells within or around areas of massive necrosis (upper columns) and micronecrosis (lower columns). Carbonic anhydrase IX is expressed in plasma membrane. Arrows indicate necrotic area. Low power view (left columns) and high power view (right columns).

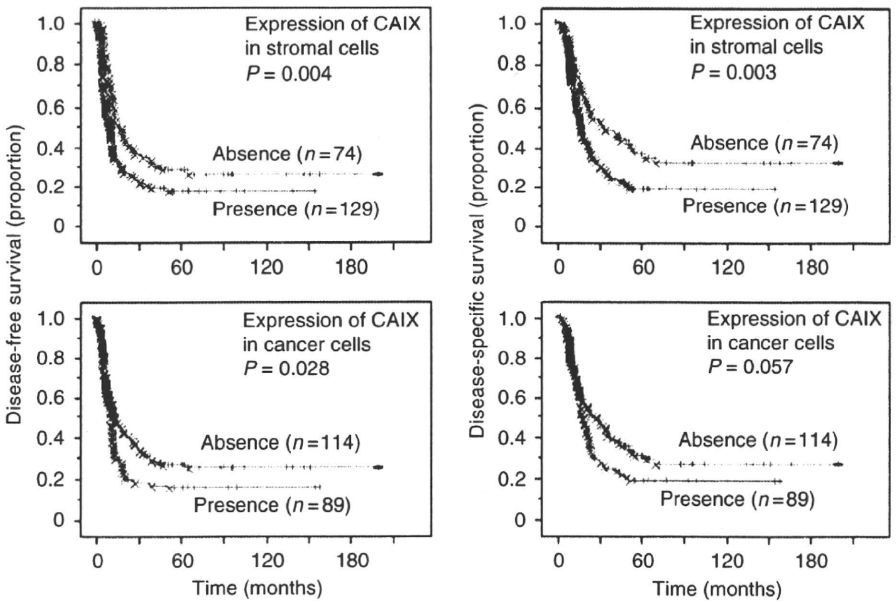

Figure 3 Kaplan–Meier survival curves showing the comparison of disease-free survival between high and low expression of CAIX (*P*-values obtained from log-rank test) (left columns). Kaplan–Meier survival curves showing the comparison of disease-specific survival between high and low expression of CAIX (*P*-values obtained from log-rank test) (right columns).

1.659–2.905) (Figure 4). A similar association was found in patients with PDC at each TNM stages (Figure 4).

The average survival periods for patients having PDC with and without necrosis were 24.62 ± 1.42 months and 47.36 ± 2.75 months, respectively. One-year survival rates for patients having PDC with and without necrosis were 63.3 ± 3.3% and 89.1 ± 2.9%, respectively; the 2-year rates were 36.2 ± 3.4% and 69.0 ± 4.3%, and the 5-year rates were 17.1 ± 2.9% and 40.1 ± 4.8%.

Multivariate Cox regression analysis showed that necrosis ($P < 0.0001$; HR = 1.853; 95% CI: 1.407–2.440), metastatic status,

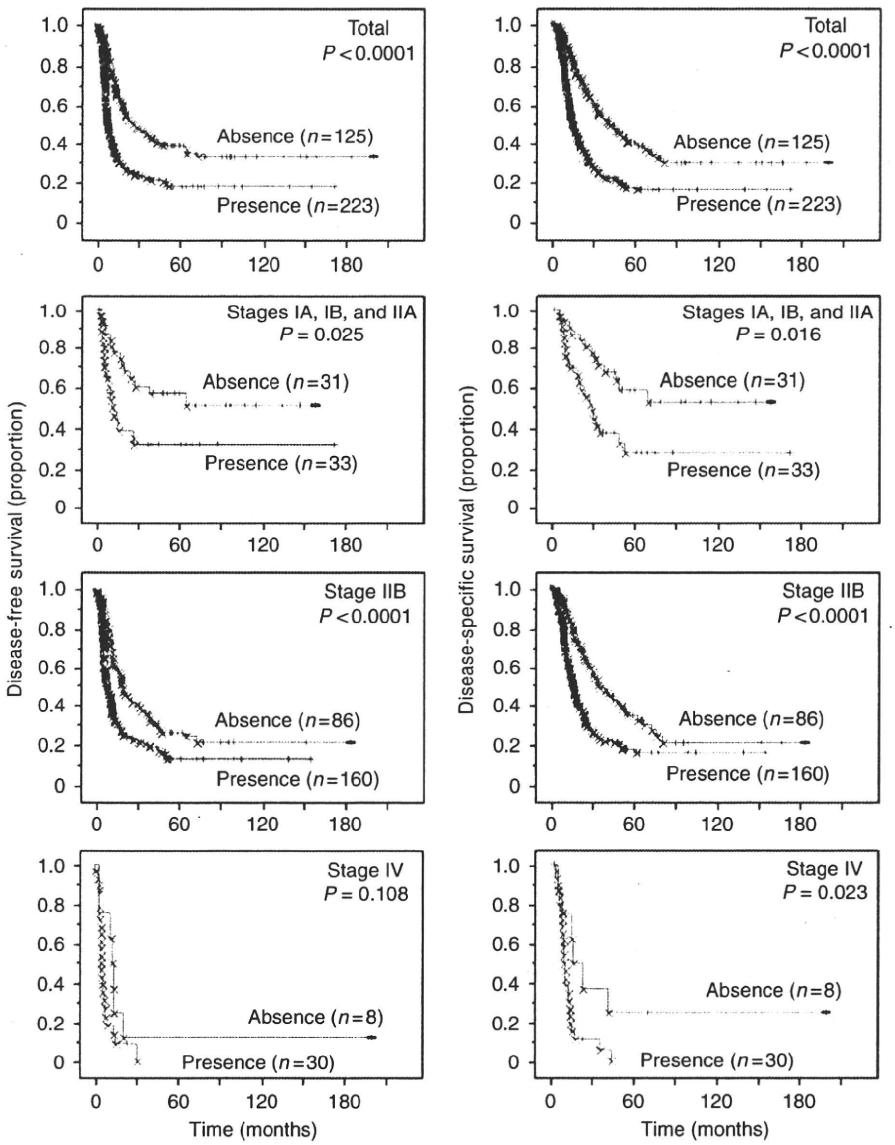

Figure 4 Kaplan–Meier survival curves showing a comparison of disease-free survival between cases in which histological necrosis was present and absent (*P*-values obtained by log-rank test) (left columns). Kaplan–Meier survival curves showing a comparison of disease-specific survival between cases, in which histological necrosis was present and absent (*P*-values obtained by log-rank test) (right columns).

lymphatic invasion, venous invasion, and intrapancreatic neural invasion were independent predictors of DFS, and that necrosis ($P<0.0001$; HR = 2.238; 95% CI: 1.686–2.971), metastatic status, margin status, lymphatic invasion, and intrapancreatic neural invasion were independent predictors of DSS (Table 2).

When massive necrosis and micronecrosis were separated as distinct variables, univariate survival analysis demonstrated an association between the presence of massive necrosis and shorter DFS ($P<0.0001$) and DSS ($P<0.0001$), and between the presence of micronecrosis and shorter DFS ($P=0.004$) and DSS ($P=0.001$) (Supplementary Table 2). Multivariate Cox regression analysis showed that massive necrosis ($P=0.0006$) and micronecrosis ($P=0.0004$) were independent predictors of shorter DFS and that massive necrosis ($P<0.0001$) and micronecrosis ($P<0.0001$) were independent predictors of shorter DSS (Supplementary Table 2).

Reproducibility of necrosis identification by independent observers

Interobserver agreement (reproducibility) regarding the identification of necrosis among the five independent observers who reviewed the 51 slides blindly had a κ-value of 0.87. On the other hand, the corresponding κ-values for grading (0–3) of lymphatic, venous, and neural invasion were 0.11, 0.11, and 0.31, respectively. According to the widely used statistical chart that grades the strength of agreement (Fleiss, 1971; Landis and Koch, 1977) into 6 categories (poor (κ-value, <0.00), slight (0.00–0.20), fair (0.21–0.40), moderate (0.41–0.60), substantial (0.61–0.80), and almost perfect (0.81–1.00)), the agreement for identification of necrosis and the grading for lymphatic, venous, and neural invasion were categorized as 'almost perfect', 'slight', 'slight', and 'fair', respectively. When the grades for lymphatic, venous, and neural

Table 2 Univariate and multivariate analyses of prognostic factors associated with disease-free survival in patients with ductal carcinoma of the pancreas ($n = 348$)

	Univariate analysis		Multivariate analysis	
Variables	**HR (95% CI)**	***P*-value**	**HR (95% CI)**	***P*-value**
Age (⩾60 years/<60 years)	1.159 (0.895–1.501)	0.263		
Gender (male/female)	0.987 (0.764–1.274)	0.919		
Localisation (pancreas head/body or tail)	0.865 (0.657–1.140)	0.304		
Tumour size (⩾30 mm/<30 mm)	1.789 (1.306–2.450)	**0.0003**		
Pathologic tumour status (T1+T2/T3)	3.863 (1.235–12.1)	**0.020**		
Pathologic node status (N0/N1)	2.028 (1.416–2.906)	**0.0001**		
Pathologic metastasis status (M0/M1)	2.258 (1.550–3.289)	**<0.0001**	2.042 (1.387–3.006)	**0.0003**
Histological grade (W/D/M/D, P/D)[a]	1.507 (1.122–2.025)	**0.006**		
Tumour margin status (negative/positive)	1.470 (1.121–1.929)	**0.005**		
PL (absence/presence)[a]	1.560 (1.182–2.060)	**0.002**		
Lymphatic invasion (0, 1/2, 3)[a]	2.040 (1.513–2.751)	**<0.0001**	1.475 (1.068–2.038)	**0.018**
Venous invasion (0, 1/2, 3)[a]	1.985 (1.508–2.614)	**<0.0001**	1.474 (1.097–1.980)	**0.010**
Intrapancreatic neural invasion (0, 1/2, 3)[a]	1.655 (1.269–2.157)	**0.0002**	1.506 (1.145–1.981)	**0.003**
Histological necrosis (absence/presence)	2.007 (1.531–2.630)	**<0.0001**	1.853 (1.407–2.440)	**<0.0001**

Univariate and multivariate analyses of prognostic factors associated with disease-specific survival in patients with ductal carcinoma of the pancreas (n = 348)

	Univariate analysis		Multivariate analysis	
Variables	**HR (95% CI)**	***P*-value**	**HR (95% CI)**	***P*-value**
Age (⩾60 years/<60 years)	1.054 (0.811–1.371)	0.692		
Gender (male/female)	0.935 (0.721–1.213)	0.615		
Localisation (pancreas head/body or tail)	0.829 (0.628–1.096)	0.189		
Tumour size (⩾30 mm/<30 mm)	1.890 (1.371–2.605)	**0.0001**		
Pathologic tumour status (T1+T2/T3)	6.333 (1.572–25.5)	**0.009**		
Pathologic node status (N0/N1)	2.024 (1.406–2.915)	**0.0002**		
Pathologic metastasis status (M0/M1)	2.199 (1.509–3.204)	**<0.0001**	1.839 (1.252–2.700)	**0.002**
Histological grade (W/D/M/D, P/D)[a]	1.611 (1.193–2.176)	**0.002**		
Tumour margin status (negative/positive)	1.555 (1.183–2.043)	**0.002**	1.379 (1.038–1.833)	**0.027**
PL (absence/presence)[a]	1.690 (1.267–2.253)	**0.0004**		
Lymphatic invasion (0, 1/2, 3)[a]	2.409 (1.762–3.293)	**<0.0001**	1.992 (1.440–2.757)	**<0.0001**
Venous invasion (0, 1/2, 3)[a]	1.968 (1.486–2.607)	**<0.0001**		
Intrapancreatic neural invasion (0, 1/2, 3)[a]	1.709 (1.305–2.238)	**<0.0001**	1.443 (1.087–1.915)	**0.011**
Histological necrosis (absence/presence)	2.196 (1.659–2.905)	**<0.0001**	2.238 (1.686–2.971)	**<0.0001**

Abbreviations: CI = confidence interval; HR = hazards ratio; M/D = moderately differentiated adenocarcinoma; P/D = poorly differentaited adenocarcinoma; PL = nerve plexus invasion; W/D = well-differentiated adenocarcinoma. [a]Classified according to the classification of pancreatic carcinoma of Japan Pancreas Society

invasion were combined into two categories (grades 0 and 1 and grades 2 and 3) as used in the survival analysis, the κ-values for lymphatic, venous, and neural invasion were 0.55 (moderate), 0.62 (substantial), and 0.62 (substantial), respectively.

Survival analysis was performed using the data for necrosis identification by the five independent observers, and this yielded similar results, that is, patients having PDC with necrosis showed significantly shorter survival. *P*-values calculated for each of these analyses were 0.0004, 0.0005, 0.002, 0.005, 0.006, and 0.008 for DFS, and 0.0001, 0.0004, 0.003, 0.005, 0.005, and 0.008 for DSS.

DISCUSSION

Pancreatic ductal carcinoma is one of the most aggressive cancers, with almost equivalent incidence and mortality rates. Several histopathological prognostic variables for patients with PDC have been reported (Trede *et al*, 1990; Yeo *et al*, 1995; Luttges *et al*, 2000; Sohn *et al*, 2000; Lim *et al*, 2003; Takai *et al*, 2003; Adsay *et al*, 2005; Mitsunaga *et al*, 2005, 2007; Shimada *et al*, 2006; Schnelldorfer *et al*, 2008). These are sometimes controversial and complex, and some have problems related to interobserver reproducibility. We need prognostic indicators being simpler, more reproducible, and accurate.

In this study, we reviewed the histopathological findings in 348 cases of PDC in comparison with the corresponding clinicopathological information, and obtained several histopathological prognosticators of both DFS and DSS for patients with PDC by univariate survival analyses employing histological necrosis, tumour size, tumour status, node status, metastatic status, margin status, nerve plexus invasion, and lymphatic, venous, and intrapancreatic neural invasion as variables. Multivariate survival analyses revealed that histological necrosis was an independent predictive factor for both shorter DFS ($P<0.0001$) and shorter DSS ($P<0.0001$) of PDC patients (Table 2). In addition, metastatic status, lymphatic invasion, venous invasion, and intrapancreatic neural invasion were factors that were independently predictive of shorter DFS, whereas metastatic status, margin status, lymphatic invasion, and intrapancreatic neural invasion were factors independently predictive of shorter DSS (Table 2). Necrosis was also able to predict patient outcome in populations at stage IIB, into which the majority of resectable PDCs were stratified (Figure 4). Furthermore, the reproducibility of necrosis identification was found to be 'almost perfect' (κ-value, 0.87) when the 51 slides of PDC were assessed by five independent observers. In contrast, the reproducibility of the systems of grading for lymphatic, venous, and neural invasion was low with low κ-values. Moreover, these five independent observers all provided the same result, that is, that patients having PDC with necrosis showed

significantly shorter survival in terms of both DFS and DSS. These findings indicate that histological necrosis is a simple, accurate, and reproducible predictor of postoperative outcome for PDC patients.

Histological necrosis was found in 223 (64.1%) out of 348 cases of PDC. We defined necrosis as covering both massive necrosis and micronecrosis, the latter being often evident in PDCs, although not noted previously or being hidden as smaller foci (Couvelard *et al*, 2005; Mitsunaga *et al*, 2005). The expression of CAIX (Figure 2) and HIF-1α (data now shown) in and around the necrotic areas was detected immunohistochemically, together with that the presence of necrosis was significantly correlated with expression of CAIX (Table 1), indicating that both patterns of necrosis were closely related to hypoxia. Hasebe's group reported that necrosis was an independent prognostic factor in both DFS and DSS when they investigated histopathological findings in 101 PDC patients (Nakatsura *et al*, 1997; Mitsunaga *et al*, 2005). Couvelard *et al* (2005) reported that necrosis was associated with poorer DSS in univariate analysis, and also showed that necrosis was significantly associated with CAIX expression. Only 30–40% of PDC cases had necrosis in those studies, whereas 60–80% of PDCs had hypoxia, as necrosis was defined roughly by these two groups as massive necrosis only.

When massive necrosis and micronecrosis were separated as distinct variables, univariate and multivariate survival analyses demonstrated that both types of necrosis were significantly associated with shorter DFS and DSS (Supplementary Table 2). Massive necrosis and micronecrosis was detected in 27.9 and 43.4% (overlapped 7.2%) of PDCs in our series, respectively. These findings suggest that the presence of necrosis, even when the lesion is small, is closely associated with patient outcome, probably because the presence of necrosis represents a hypoxia-associated aggressive tumour phenotype. In fact, in this series, the presence of necrosis was significantly correlated with a large tumour size, higher T factor, presence of nodal and distant metastasis, higher TNM stage, more severe venous invasion, and a higher tumour histological grade (Table 1), suggesting that necrosis is positively correlated with tumour growth, invasion, and angiogenesis, that is, an aggressive phenotype.

Hypoxia is a characteristic of invasive cancers that can lead to the development of an aggressive phenotype through a mechanism mediated mainly by HIF-1α, which includes cell immortalisation and dedifferentiation, pH regulation, autocrine growth/survival, angiogenesis, invasion/metastasis, and resistance to chemotherapy (Semenza, 2006, 2009; Grothey and Galanis, 2009). In fact, the presence of hypoxic foci with expression of CAIX was an independent worse prognostic factor for PDC patients (Supplementary Table 1) that we demonstrated at first time using large series of cases. Recently, HIF-1 targeting therapy and anti-angiogenesis therapy have been reported to yield promising anti-cancer effects (Sessa *et al*, 2008; Grothey and Galanis, 2009; Semenza, 2009). It is suggested that evaluation of histological necrosis would be useful not only for decision making about postoperative clinical management, but also for stratifying patients for clinical trials aimed at evaluating HIF-1 targeting or anti-angiogenesis therapies.

In conclusion, we reviewed the histopathological findings in 348 PDCs for which the presence of necrosis was redefined, and found that histological necrosis was an independent predictor of shorter DFS and DSS for the affected patients. Interobserver reproducibility for the detection of necrosis was assessed as 'almost perfect' when 51 slides of PDC were reviewed by five independent observers. These findings indicate that histological necrosis is a simple, accurate, and reproducible predictor of postoperative outcome in PDC patients.

ACKNOWLEDGEMENTS

Research support: This work was supported by a Grant-in-Aid for Third Term Comprehensive 10-year Strategy for Cancer Control from the Ministry of Health, Labor and Welfare of Japan (NH and YK), the Program for Promotion of Fundamental Studies in Health Sciences of the National Institute of Biomedical Innovation (YK), and a Grant-in-Aid for Scientific Research from the Ministry of Education, Culture, Sports, Science and Technology of Japan (NH). The authors thank Dr Hidenori Ojima, Dr Yoshihiro Sakamoto, Dr Minoru Esaki, and Dr Satoshi Nara for useful discussion.

Supplementary Information accompanies the paper on British Journal of Cancer website (http://www.nature.com/bjc)

REFERENCES

Adsay NV, Basturk O, Bonnett M, Kilinc N, Andea AA, Feng J, Che M, Aulicino MR, Levi E, Cheng JD (2005) A proposal for a new and more practical grading scheme for pancreatic ductal adenocarcinoma. *Am J Surg Pathol* **29:** 724–733

Bristow RG, Hill RP (2008) Hypoxia and metabolism. Hypoxia, DNA repair and genetic instability. *Nat Rev Cancer* **8:** 180–192

Center for Cancer Control and Information Services, National Cancer Center Japan (2009) Cancer Statistics in Japan

Chia SK, Wykoff CC, Watson PH, Han C, Leek RD, Pastorek J, Gatter KC, Ratcliffe P, Harris AL (2001) Prognostic significance of a novel hypoxia-regulated marker, carbonic anhydrase IX, in invasive breast carcinoma. *J Clin Oncol* **19:** 3660–3668

Couvelard A, O'Toole D, Leek R, Turley H, Sauvanet A, Degott C, Ruszniewski P, Belghiti J, Harris AL, Gatter K, Pezzella F (2005) Expression of hypoxia-inducible factors is correlated with the presence of a fibrotic focus and angiogenesis in pancreatic ductal adenocarcinomas. *Histopathology* **46:** 668–676

Fleiss JL (1971) Measuring nominal scale agreement among many rates. *Pshycol Bull* **76:** 378–382

Gilchrist KW, Gray R, Fowble B, Tormey DC, Taylor SGt (1993) Tumor necrosis is a prognostic predictor for early recurrence and death in lymph node-positive breast cancer: a 10-year follow-up study of 728 Eastern Cooperative Oncology Group patients. *J Clin Oncol* **11:** 1929–1935

Grothey A, Galanis E (2009) Targeting angiogenesis: progress with anti-VEGF treatment with large molecules. *Nat Rev Clin Oncol* **6:** 507–518

Harris AL (2002) Hypoxia – a key regulatory factor in tumour growth. *Nat Rev Cancer* **2:** 38–47

Hruban RH, Pitman MB, Klimstra DS (2007) Ductal adenocarcinoma. In *AFIP Atlas of Tumor Pathology. Tumors of the Pancreas*, Hruban RH, Pitman MB, Klimstra DS (eds) 4th edn, pp 111–164. ARP Press: Washington, DC

Japan Pancreas Society (2003) *Classification of Pancreatic Cancer.* 2nd English edn, Kanehara: Tokyo, Japan

Jemal A, Siegel R, Ward E, Hao Y, Xu J, Thun MJ (2009) Cancer statistics, 2009. *CA Cancer J Clin* **59:** 225–249

Kitada T, Seki S, Sakaguchi H, Sawada T, Hirakawa K, Wakasa K (2003) Clinicopathological significance of hypoxia-inducible factor-1alpha expression in human pancreatic carcinoma. *Histopathology* **43:** 550–555

Klöppel G, Adler G, Hruban RH, Kern SE, Longnecker DS, Partanen TJ (2000) Ductal adenocarcinoma of the pancreas. In *World Health Organization Classification of Tumours. Pathology & Genetics. Tumours of the Digestive System*, Hamilton SR, Aaltonen LA (eds), pp 221–230. IARC Press: Lyon

Landis JR, Koch GG (1977) The measurement of observer agreement for categorical data. *Biometrics* **33:** 159–174

Lim JE, Chien MW, Earle CC (2003) Prognostic factors following curative resection for pancreatic adenocarcinoma: a population-based, linked database analysis of 396 patients. *Ann Surg* **237:** 74–85

Luttges J, Schemm S, Vogel I, Hedderich J, Kremer B, Klöppel G (2000) The grade of pancreatic ductal carcinoma is an independent prognostic factor and is superior to the immunohistochemical assessment of proliferation. *J Pathol* **191:** 154–161

Mitsunaga S, Hasebe T, Iwasaki M, Kinoshita T, Ochiai A, Shimizu N (2005) Important prognostic histological parameters for patients with invasive ductal carcinoma of the pancreas. *Cancer Sci* **96:** 858–865

Mitsunaga S, Hasebe T, Kinoshita T, Konishi M, Takahashi S, Gotohda N, Nakagohri T, Ochiai A (2007) Detail histologic analysis of nerve plexus invasion in invasive ductal carcinoma of the pancreas and its prognostic impact. *Am J Surg Pathol* **31:** 1636–1644

Nakatsura T, Hasebe T, Tsubono Y, Ryu M, Kinoshita T, Kawano N, Konishi M, Kosuge T, Kanai Y, Mukai K (1997) Histological prognostic parameters for adenocarcinoma of the pancreatic head. Proposal for a scoring system for prediction of outcome. *J Hep Bil Pancr Surg* **4:** 441–448

Ord JJ, Agrawal S, Thamboo TP, Roberts I, Campo L, Turley H, Han C, Fawcett DW, Kulkarni RP, Cranston D, Harris AL, Ord JJ, Agrawal S, Thamboo TP, Roberts I, Campo L, Turley H, Han C, Fawcett DW, Kulkarni RP, Cranston D, Harris AL (2007) An investigation into the prognostic significance of necrosis and hypoxia in high grade and invasive bladder cancer. *J Urol* **178:** 677–682

Pastorekova S, Zavadova Z, Kostal M, Babusikova O, Zavada J (1992) A novel quasi-viral agent, MaTu, is a two-component system. *Virology* **187:** 620–626

Philip PA, Mooney M, Jaffe D, Eckhardt G, Moore M, Meropol N, Emens L, O'Reilly E, Korc M, Ellis L, Benedetti J, Rothenberg M, Willett C, Tempero M, Lowy A, Abbruzzese J, Simeone D, Hingorani S, Berlin J, Tepper J (2009) Consensus report of the national cancer institute clinical trials planning meeting on pancreas cancer treatment. *J Clin Oncol* **27:** 5660–5669

Schnelldorfer T, Ware AL, Sarr MG, Smyrk TC, Zhang L, Qin R, Gullerud RE, Donohue JH, Nagorney DM, Farnell MB (2008) Long-term survival after pancreatoduodenectomy for pancreatic adenocarcinoma: is cure possible? *Ann Surg* **247:** 456–462

Semenza GL (2006) Development of novel therapeutic strategies that target HIF-1. *Expert Opin Ther Targets* **10:** 267–280

Semenza GL (2009) HIF-1 inhibitors for cancer therapy: from gene expression to drug discovery. *Curr Pharm Des* **15:** 3839–3843

Sessa C, Guibal A, Del Conte G, Ruegg C (2008) Biomarkers of angiogenesis for the development of antiangiogenic therapies in oncology: tools or decorations? *Nat Clin Pract Oncol* **5:** 378–391

Shimada K, Sakamoto Y, Sano T, Kosuge T, Hiraoka N (2006) Reappraisal of the clinical significance of tumor size in patients with pancreatic ductal carcinoma. *Pancreas* **33:** 233–239

Sohn TA, Yeo CJ, Cameron JL, Koniaris L, Kaushal S, Abrams RA, Sauter PK, Coleman J, Hruban RH, Lillemoe KD (2000) Resected adenocarcinoma of the pancreas-616 patients: results, outcomes, and prognostic indicators. *J Gastrointest Surg* **4:** 567–579

Sun HC, Qiu ZJ, Liu J, Sun J, Jiang T, Huang KJ, Yao M, Huang C, Sun H-C, Qiu Z-J, Liu J, Sun J, Jiang T, Huang K-J, Yao M, Huang C (2007) Expression of hypoxia-inducible factor-1 alpha and associated proteins in pancreatic ductal adenocarcinoma and their impact on prognosis. *Int J Oncol* **30:** 1359–1367

Takahashi Y, Akishima-Fukasawa Y, Kobayashi N, Sano T, Kosuge T, Nimura Y, Kanai Y, Hiraoka N (2007) Prognostic value of tumor architecture, tumor-associated vascular characteristics, and expression of angiogenic molecules in pancreatic endocrine tumors. *Clin Cancer Res* **13:** 187–196

Takai S, Satoi S, Toyokawa H, Yanagimoto H, Sugimoto N, Tsuji K, Araki H, Matsui Y, Imamura A, Kwon AH, Kamiyama Y (2003) Clinicopathologic evaluation after resection for ductal adenocarcinoma of the pancreas: a retrospective, single-institution experience. *Pancreas* **26:** 243–249

Trede M, Schwall G, Saeger HD (1990) Survival after pancreatoduodenectomy. 118 consecutive resections without an operative mortality. *Ann Surg* **211:** 447–458

Vaupel P, Mayer A (2007) Hypoxia in cancer: significance and impact on clinical outcome. *Cancer Metastasis Rev* **26:** 225–239

Wittekind C, Greene FL, Hutter RVP, Klimpfinger M, Sobin LH (2005) *UICC TNM Atlas* 5th edn, Springer: New York, NY

Yeo CJ, Cameron JL, Lillemoe KD, Sitzmann JV, Hruban RH, Goodman SN, Dooley WC, Coleman J, Pitt HA (1995) Pancreaticoduodenectomy for cancer of the head of the pancreas. 201 patients. *Ann Surg* **221:** 721–731; discussion 731–733

Zavada J, Zavadova Z, Pastorek J, Biesova Z, Jezek J, Velek J (2000) Human tumour-associated cell adhesion protein MN/CA IX: identification of M75 epitope and of the region mediating cell adhesion. *Br J Cancer* **82:** 1808–1813

Cancer Science
The official journal of the Japanese Cancer Association JCA

Establishment of six new human biliary tract carcinoma cell lines and identification of MAGEH1 as a candidate biomarker for predicting the efficacy of gemcitabine treatment

Hidenori Ojima,[1] Daitaro Yoshikawa,[2] Yoshihiro Ino,[1] Hiroko Shimizu,[2] Masashi Miyamoto,[2] Akiko Kokubu,[2] Nobuyoshi Hiraoka,[1] Noriaki Morofuji,[3] Tadashi Kondo,[3] Hiroaki Onaya,[4] Takuji Okusaka,[5] Kazuaki Shimada,[6] Yoshihiro Sakamoto,[6] Minoru Esaki,[6] Satoshi Nara,[6] Tomoo Kosuge,[6] Setsuo Hirohashi,[1,2] Yae Kanai[1] and Tatsuhiro Shibata[1,2,7]

[1]Pathology Division, [2]Cancer Genomics Project, [3]Proteome Bioinformatics Project, National Cancer Center Research Institute, Chuo-ku, Tokyo; [4]Diagnostic Radiology Section, Clinical Trials and Practice Support Division, Center for Cancer Control and Information Services, National Cancer Center, Chuo-ku, Tokyo; [5]Hepatobiliary and Pancreatic Oncology Division, [6]Hepatobiliary and Pancreatic Surgery Division, National Cancer Center Hospital, Chuo-ku, Tokyo, Japan

(Received October 6, 2009/Revised November 25, 2009; December 1, 2009/Accepted December 1, 2009/Online publication January 21, 2010)

The aim of this study was to establish new biliary tract carcinoma (BTC) cell lines and identify predictive biomarkers for the potential effectiveness of gemcitabine therapy. Surgical specimens of BTC were transplanted directly into immunodeficient mice to establish xenografts, then subjected to *in vitro* cell culture. The gemcitabine sensitivity of each cell line was determined and compared with the genome-wide gene expression profile. A new predictive biomarker candidate was validated using an additional cohort of gemcitabine-treated BTC cases. From 55 BTC cases, we established 19 xenografts and six new cell lines. Based on their gemcitabine sensitivity, 10 BTC cell lines (including six new and four publicly available ones) were clearly categorized into two groups, and MAGEH1 mRNA expression in the tumor cells showed a significant negative correlation with their sensitivity to gemcitabine. Immunohistochemically, MAGEH1 protein was detected in three (50%) out of six sensitive cell lines, and four (100%) out of four resistant cell lines. In the validation cohort of gemcitabine-treated recurrence cases, patients were categorized into "effective" and "non-effective" groups according to the RECIST guidelines for assessment of chemotherapeutic effects. MAGEH1 protein expression was detected in two (40%) out of five "effective" cases and all four (100%) "non-effective" cases. We have established a new BTC bioresource that covers a wide range of biological features, including drug sensitivity, and is linked with clinical information. Negative expression of MAGEH1 protein serves as a potential predictive marker for the effectiveness of gemcitabine therapy in BTC. (*Cancer Sci* 2010; 101: 882–888)

Biliary tract carcinoma (BTC) has a poor prognosis, and most cases are diagnosed at advanced stages when patients present with overt symptoms. Previous studies have reported that surgical resection is the only curative treatment for BTC patients,[1–4] and no standard chemotherapy regimens have been established for inoperable cases or cases of recurrence after surgical resection.[5,6] Exceptionally, gemcitabine (2′-deoxy-2′-difluorodeoxycytidine), a deoxycytidine analog with structural and metabolic similarities to cytarabine, has been reported to be clinically effective and is considered a first-line chemotherapy for BTC, although its associated response rates (8–60%) and median overall survival (6.3–16 months) are not satisfactory.[7] It has been reported that both intrinsic and acquired resistance are important factors in the failure of gemcitabine treatment in patients with pancreatic cancer.[8] However, there have been few attempts to clarify the molecular mechanisms of gemcitabine resistance, and no data are currently available for BTC.

One factor preventing better understanding of drug resistance at the cellular and molecular levels in BTC is that only a few BTC cell lines are available for such analyses. Additionally, the construction and utility of an animal experimental model is essential for validating the *in vitro* data for these cell lines, but no such model has been established. Therefore, there is an urgent need to establish BTC cell lines from a wide range of clinical cases and apply them for translational research aimed at connecting basic research with clinical trials. In the present study, we successfully prepared 19 xenograft models from surgically resected BTC samples, and established six new cell lines. Using these new resources, we searched for molecular biomarkers associated with gemcitabine sensitivity. We also validated the efficacy of one candidate molecule, MAGEH1, as a surrogate biomarker of gemcitabine response by immunohistochemical analysis of an additional clinical cohort of gemcitabine-treated BTC.

Materials and Methods

Establishment of xenografts and tumor cell lines. The study included 55 patients with BTC who underwent radical surgery with curative intent at the National Cancer Center Hospital (Tokyo, Japan) between 2005 and 2008. The main tumor nodule was located in the lower, middle, and upper thirds of the extrahepatic bile duct, the hilar bile duct, and intrahepatic area in 4, 11, 2, 4, and 34 patients, respectively. Tumor specimens were transported to the Surgical Pathology department immediately after surgical resection, and tissue in excess of that needed for diagnosis was used for this study. The tumor tissues were washed in physiological saline, cut into small pieces (2–4 mm^3 fragments), then implanted subcutaneously into SCID mice. Congenital athymic female C.B17/Icr-scid(scid/scid) mice (CLEA Japan, Tokyo, Japan), 5–7 weeks old, were bred and housed under specific pathogen-free conditions at the National Cancer Center Research Institute Animal Center. Tumor growth to a size of 1–2 cm after maintaining the animals for 1–2 months was regarded as engraftment, and the tumors were passaged a maximum of three to five times. Xenografts in mice were passaged similarly to the transplantation of surgical

[7]To whom correspondence should be addressed. E-mail: tashibat@ncc.go.jp

doi: 10.1111/j.1349-7006.2009.01462.x

specimens, and the tumors were subjected to cell culture after each passage. For establishment of cell lines, the xenograft tumor tissues were washed in Isozin (Meiji, Tokyo, Japan) and physiological saline, cut into small pieces, then plated into 6 cm dishes containing RPMI medium supplemented with 10% FC), 2 mM L-glutamine, 100 mg/mL streptomycin sulfate, and 100 ID/mL penicillin G sodium. Some surgical specimens were directly subjected to cell line preparation. Contaminating fibroblasts were periodically removed by wiping under microscopic observation. The cells were incubated at 37°C in 5% CO_2 in air, and the medium was changed once or twice a week. A solution of 0.05% trypsin and 0.53 mM EDTA (1×; Gibco™/Invitrogen Corporation, Carlsbad, CA, USA) was used for passaging the cells (1:3 split). Each cell line underwent repeated passage more than 20 times. Established cell lines were implanted subcutaneously into SCID mice to make xenografts for further analyses.

Mice were kept at the Animal Care and Use Facilities of the National Cancer Center (Tokyo, Japan) under specific pathogen-free conditions. All experiments were approved by the Animal Care and Ethics Committee of the National Cancer Center. This study was approved by the Ethical Committee of the National Cancer Center.

Biliary tract carcinoma cell lines obtained from cell banks. Four human BTC cell lines derived from Japanese patients (TKKK, OZ, TGBC24TKB, and HuCCT1) were purchased from Riken Bioresource Center (Tsukuba, Japan) or from the Japanese Collection of Research Bioresources (Osaka, Japan). The TKKK cell line was derived from intrahepatic cholangiocarcinoma, and the OZ, TGBC24TKB, and HuCCT1 cell lines from extrahepatic bile duct carcinoma.

Chemicals. Gemcitabine was obtained from Eli Lilly Pharmaceuticals (Indianapolis, IN, USA). All other chemicals were of analytical grade and commercially available.

Cytotoxicity assays for gemcitabine. The cytotoxicity of gemcitabine for each cell line was assessed by a modified 3-(4,5-dimethylthiazol-2-yl)-5-(3-carboxymethoxyphenyl)-2-(4-sulfophenyl)-2H-tetrazolium, inner salt assay with CellTiter 96 AQueous One Solution Reagent (Promega, Madison, WI, USA). Tumor cells (2000 cells/well) in the exponential growth phase were grown in 96-well plates. Twenty-four hours after plating, the cells were incubated in the presence of each concentration (0 (control)–100 μM) of gemcitabine for another 72 h at 37°C in a humidified atmosphere of 5% CO_2 in air. After treatment, 20 μL CellTiter 96 AQueous One Solution Reagent was dropped into each well in the plates and the absorbance at 490 nm was recorded. Absorbance values were expressed as a percentage of untreated controls, and IC_{50} was calculated.

Gene expression analysis. Total RNA was extracted from 10 BTC cell lines using an RNeasy Micro Kit (Qiagen, Velencia, CA, USA) in accordance with the manufacturer's instructions. The total RNA yields and purity were determined spectrophotometrically by measuring the absorbance of aliquots at 260 and 280 nm. cDNA and Cy3-labeled cRNA were synthesized using a Quick Amp Labeling Kit (Agilent Technologies, Santa Clara, CA, USA). The labeled cRNA probe was hybridized to an oligonucleotide microarray (Whole Human Genome 44K Array; Agilent Technologies) covering more than 41 000 human transcripts. Array hybridization and washing were carried out according to the recommended protocols, and microarrays were scanned using a DNA Microarray Scanner (Agilent Technologies) and analyzed using Gene Spring software (Agilent Technologies).

Quantitative RT-PCR. One microgram of total RNA was converted to cDNA using a Transcriptor First Strand cDNA Synthesis Kit (Roche, Basel, Switzerland) in accordance with the manufacturer's instructions. Quantitative RT-PCR (qRT-PCR) was carried out using LightCycler 480 (Roche) in accordance with the manufacturer's instructions. For standardization of the amount of RNA, expression of GAPDH in each sample was quantified. (Primers are shown in Table S1.)

Mutation analysis of *p53* and *KRAS* genes. Each exon of the *p53* and *KRAS* genes (exons 5–8 of *p53* and exons 1–2 of *KRAS*) was amplified from genomic DNA of each cell line and gel-purified. Direct sequencing was carried out using a BigDye Terminator v3.1 Cycle Sequencing Kit (Applied Biosystems, Foster City, California, USA). (Primers are shown in Table S1.)

Assessment of response to gemcitabine in cases of recurrent BTC. Among the 100 patients who underwent surgery for BTC between September 26, 2003, and October 2, 2007, 34 developed recurrent tumors and received chemotherapy, and were followed for 6 months or longer. Among these patients, 24 who were treated with gemcitabine alone were selected for this study. The mean duration of postoperative follow-up in these 24 patients was 627 days. We further excluded 15 patients from the analysis because: (i) the drug administration period was less than 1 month in three patients; (ii) the diagnosis of tumor recurrence was not consistent between the oncologist and the radiologist in three patients; (iii) we were unable to obtain an accurate judgement of the efficacy of gemcitabine treatment in five patients; (iv) the histological diagnosis was an uncommon type of adenocarcinoma (bile duct cystadenocarcinoma, solid adenocarcinoma, and combined carcinoma) in three patients; and (v) preoperative therapy (radiation therapy) had been carried out in one patient. The effect of chemotherapy was assessed by an oncologist and a radiologist (T.O. and H.O., respectively) in accordance with the RECIST guidelines for assessment of chemotherapeutic effects.[9] None of the patients was judged as showing a complete response or a partial response. The effect of chemotherapy was categorized as "effective" or "non-effective". The "effective" group included patients whose efficacy state was stable disease for 6 months or more during chemotherapy. The "non-effective" group included patients whose efficacy state was stable disease for 5 months or less, or progressive disease during chemotherapy.

Immunohistochemical reactivity of MAGEH1 in human tumor xenografts and surgically resected specimens. Immunohistochemical analysis of MAGEH1 expression on formalin-fixed, paraffin-embedded sections of tumor xenograft tissues and surgical specimens was done using the polymer-based method (Envision+Dual Link System-HRP; Dako, Glostrup, Denmark) in accordance with the manufacturer's instructions. For antigen retrieval, the sections were autoclaved in 10 mM citrate buffer (pH 6.0) at 121°C for 10 min. We used a rabbit anti-MAGEH1 polyclonal antibody (ab64784; Abcom, Cambridge, Massachusetts, USA) at a dilution of 1:500. Staining intensity was independently evaluated by two pathologists (H.O. and T.S.) without knowledge of the clinical data. Using the expression in normal hepatocytes or pancreatic duct epithelial cells as a positive control, we classified cases as MAGEH1-positive when more than 50% of tumor cells were positively stained. If the tumor showed varying degrees of differentiation, staining intensity was evaluated in the area with the most dominant type of differentiation.

Statistical analysis. The unpaired *t*-test was used for assessment of the microarray data. Microarray and qRT-PCR data were analyzed by Pearson's correlation test.

Results

Establishment and characterization of BTC xenografts and cell lines. To establish useful BTC resources, we subcutaneously transplanted 55 BTC samples (4, 11, 2, 4, and 34 cases of lower, middle, and upper thirds of the extrahepatic bile duct carcinoma, hilar bile duct carcinoma, and intrahepatic cholangiocarcinoma, respectively) into 435 immunocompromised (SCID) mice.

Table 1. Clinicopathological features of original biliary tract tumors

Xenograft	Pathological diagnosis of original tumor	Age (years)/Sex	Histologic type	Prognosis (Survival [days])	Cell line
1	CCC	70/F	Adeno, mod	Death (402)	NCC-CC1
2	CCC	71/F	Adeno, mod	Death (175)	NCC-CC3-1/-2
3	CCC	59/M	Adeno, mod	Alive (219)	NCC-CC4-1
4	Middle BDCa	58/F	Adeno, mod	Death (299)	NCC-BD1
5	Lower BDCa	77/F	Adeno, mod	Alive (316)	NCC-BD2
6	Hilar BDCa	48/M	Adeno, well	Death (500)	NA
7	CCC	54/F	Adeno, mod	Death (181)	NA
8	CCC	56/M	Adeno, mod	Death (319)	NA
9	CCC	73/M	Adeno, mod	Death (53)	NA
10	CCC	54/M	Adeno, mod	Alive (655)	NA
11	CCC	45/F	Adeno, mod	Alive (623)	NA
12	CCC	72/M	Muc	Alive (647)	NA
13	Middle BDCa	54/M	Adeno, mod	Alive (535)	NA
14	CCC	69/M	Adeno, mod	Death (174)	NA
15	Hilar BDCa	70/M	Adeno, mod	Alive (355)	NA
16	Middle BDCa	67/M	Adeno, mod	Alive (450)	NA
17	CCC	78/M	Adeno, mod	Alive (299)	NA
18	Middle BDCa	66/F	Adeno, mod	Alive (198)	NA
19	CCC	66/M	Adeno, mod	Death (168)	NA

Adeno, adenocarcinoma; CCC, cholangiocellular carcinoma; F, female; hilar BDCa, hilar bile duct carcinoma; lower BDCa, lower third of extrahepatic bile duct carcinoma; M, male; middle BDCa, middle third of extrahepatic bile duct carcinoma; mod, moderately differentiated; muc, mucinous adenocarcinoma; well, well differentiated; NA, not applicable.

Table 2. Mutation status of *p53* and *KRAS* genes of established novel biliary tract carcinoma cell lines

Cell line	*KRAS* (exons 1–2)		*p53* (exons 5–8)	
	Nucleotide change	Amino acid change	Nucleotide change	Amino acid change
NCC-BD1	G37C	G13C	C457T, A463C,G467C	P153S, T155P, R156P
NCC-BD2	WT	WT	Homozygous deletion	No product
NCC-CC1	G35T	G12V	G524A	R175H
NCC-CC3-1	G35A	G12D	WT	WT
NCC-CC3-2	G35A	G12D	WT	WT
NCC-CC4-1	WT	WT	WT	WT

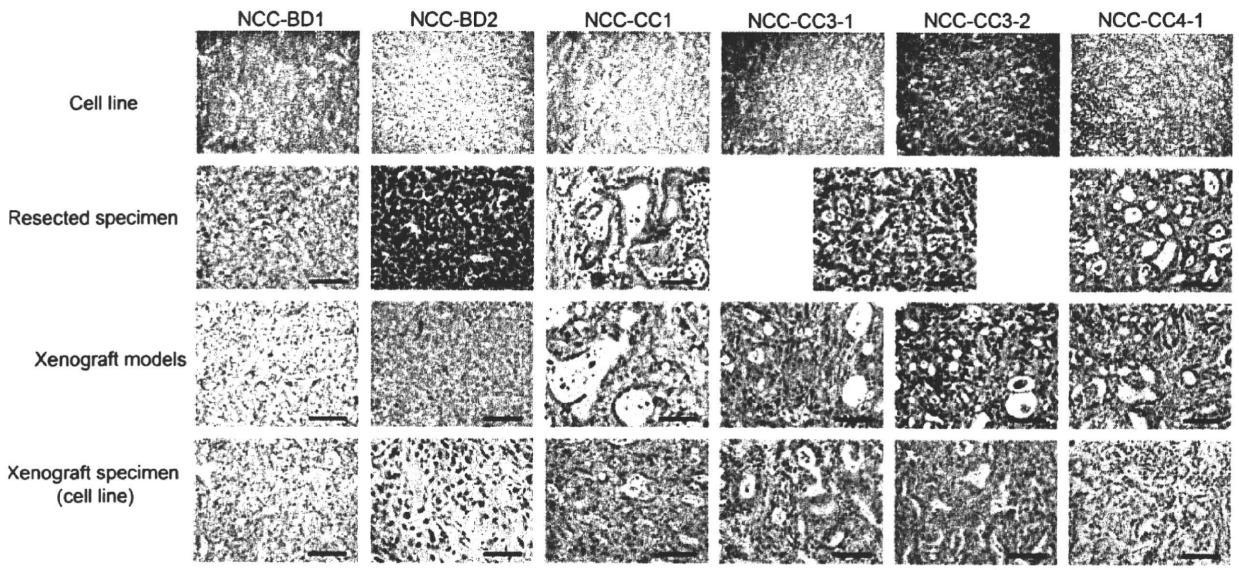

Fig. 1. Cell morphology and tumor histology of primary specimen/xenograft of established new biliary tract carcinoma cell lines. *In vitro* cell morphology and tumor histology (H&E staining) of resected primary specimens, xenografts of primary tumor samples and xenografts of cell lines are shown. Scale line = 200 μm.

doi: 10.1111/j.1349-7006.2009.01462.x

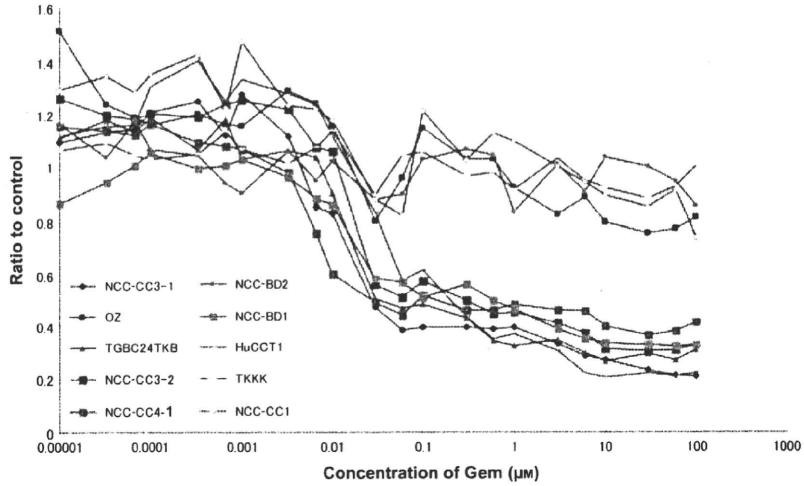

Fig. 2. Sensitivity to gemcitabine (Gem) in 10 biliary tract carcinoma cell lines. Ratio of cell proliferation compared to the control (treated with DMSO) at each concentration (μM) of Gem was plotted. Note that 10 cell lines are clearly segregated into two groups (Gem-sensitive and Gem-resistant) with distinct Gem sensitivity.

Nineteen xenograft models (1, 4, 0, 2, and 12 cases of lower, middle, and upper thirds of the extrahepatic bile duct carcinoma, hilar bile duct carcinoma, and intrahepatic cholangiocarcinoma, respectively) were obtained, and six cell lines including two subclones were established through xenograft models (five cell lines) or directly from a surgical specimen (one cell line). The cell lines were designated as NCC-BD1, NCC-BD2, NCC-CC1, NCC-CC3-1, NCC-CC3-2, and NCC-CC4-1, respectively. Four cell lines were derived from intrahepatic BTC and two from extrahepatic BTC (Table 1). Other clinicopathological features of the patients from whom the cell lines were obtained are summarized in Table 1.

Mutation analysis of the *KRAS* and *p53* genes revealed frequent (3/5, 60%) alterations in them. It also confirmed that these new cell lines were of human origin and that two subclones, NCC-CC3-1 and NCC-CC3-2, shared the same *KRAS* mutation (Table 2). The morphology and histology of the established cell lines and primary tumors, and xenografts of primary tumor and cell lines, are shown in Figure 1. As NCC-BD2 cells were unable to form tumors in mice, we used a cell block of this cell line. Comparing the morphological features between primary tumors and cell lines, we observed considerable conservation of tumor histology (Fig. 1), suggesting that the established cell lines could be considered representative of each original primary.

Classification of 10 BTC cell lines by gemcitabine sensitivity. We then attempted to evaluate whether these new cell lines could be used for revealing novel biomarkers for drug sensitivity. For this purpose, we first determined the gemcitabine sensitivity of 10 BTC cell lines including four commercially available BTC cell lines. The relative survival ratios of the 10 BTC cell lines in response to various doses of gemcitabine are shown in Figure 2. The IC_{50} value for each cell line was calculated, and the results are summarized in Table 3. Interestingly, as can be seen in Figure 2, on the basis of drug sensitivity, we were able to classify these cell lines into two groups: a gemcitabine-sensitive group that included NCC-BD1, NCC-CC3-1, NCC-CC3-2, NCC-CC4-1, HuCCT1, and TGBC24TKB cells (the IC_{50} values being 0.6, 0.03, 0.06, 0.03, 0.2, and 0.03 μM respectively) and a gemcitabine-resistant group that included NCC-BD2, NCC-CC1, TKKK, and OZ cells, whose IC_{50} values were beyond the range of our measurement (>100 μM). As all of the newly established cell lines were from chemotherapy-naïve tumors, this result suggests that BTC cells possess intrinsic molecular mechanism associated with gemcitabine sensitivity.

Significant differences in mRNA expression between groups sensitive and resistant to gemcitabine. To further elucidate the molecular differences between the groups sensitive and resistant to gemcitabine, we investigated the genome-wide mRNA expression in all the cell lines. By comparing the sensitive group with the resistant group, we isolated genes that showed significant differences in expression between the two (Table 4). These included genes associated with cell signaling (*SEC23A*, *RRAS2*, and *BMP8B*) or telomere maintenance (*TERF1*), or genes whose functions were unknown (*NOL10*, *CCDC117*, and *ZSWIM6*). All were candidate biomarkers associated with gemcitabine sensitivity, and among them we focused on MAGEH1 (melanoma antigen family H 1) because: (i) mRNA expression of MAGEH1 in the resistant group was more than five times higher than in the sensitive group; (ii) MAGEH1 is a transmembrane protein that is easily accessible to antibody; and (iii) there was a significant difference in its expression between the two groups ($P = 0.000093$). We then validated the differential expression of MAGEH1 between the two groups by qRT-PCR. As shown in Figure 3, the data for MAGEH1 expression obtained by qRT-PCR, which was normalized with GAPDH expression, was highly correlated with DNA microarray data (coefficient of correlation, 0.847) and also differed significantly ($P = 0.009$) between the sensitive and resistant groups.

MAGEH1 expression in gemcitabine-treated BTC cases. Finally, we tested whether MAGEH1 expression is correlated with clinical response to gemcitabine treatment by immunohistochemical analysis of clinical cases. Before analyzing the clinical samples, we tested the anti-MAGEH1 antibody in xenograft tumor samples. Three cell lines (50%) out of the six sensitive cell lines and

Table 3. Gemcitabine IC_{50} values and assessment of reactive cytotoxicity of biliary tract carcinoma cell lines

Cell line	IC_{50} (μM)	Drug sensitivity
NCC-BD1	0.60	S
NCC-BD2	>100	R
NCC-CC1	>100	R
NCC-CC3-1	0.03	S
NCC-CC3-2	0.06	S
NCC-CC4-1	0.03	S
TKKK	>100	R
OZ	>100	R
Hucct1	0.20	S
TGBC24TKB	0.03	S

R, resistant; S, sensitive.

Table 4. List of genes differentially expressed between gemcitabine sensitive and resistant groups of biliary tract carcinoma cell lines

Gene symbol	Average expression (R)	Average expression (S)	Ratio (R/S)	*P*-value†	Chromosome locus
TIMELESS	1.866235575	0.858141402	2.174741332	1.45E-05	12q12-q13
SEC23A	1.601411675	0.796303448	2.011057064	2.34E-05	14q21.1
MAGEH1	2.100036325	0.397001692	5.289741503	9.28E-05	Xp11.21
NOL10	1.482213925	0.854618707	1.734356987	0.000201766	2p25.1
RRAS2	0.221456871	1.54467481	0.143367956	0.000429397	11p15.2
BMP8B	1.7544659	0.572194878	3.066203432	0.000440394	1p35-p32
TERF1	1.422439425	0.778783987	1.826487767	0.000451224	8q13
SEC23A	1.5599122	0.633786226	2.461259234	0.0004951	14q21.1
CCDC117	1.71272665	0.699035142	2.45012954	0.000557389	22q12.1
C14orf107	0.490823853	1.299093433	0.377820286	0.000632072	14q22.3
ZSWIM6	0.508965063	1.33793895	0.380409781	0.000753833	5q12.1
RPL34	0.52856332	1.102003908	0.479638335	0.000934328	4q25

†Obtained using the unpaired *t*-test. R, resistant group; S, sensitive group.

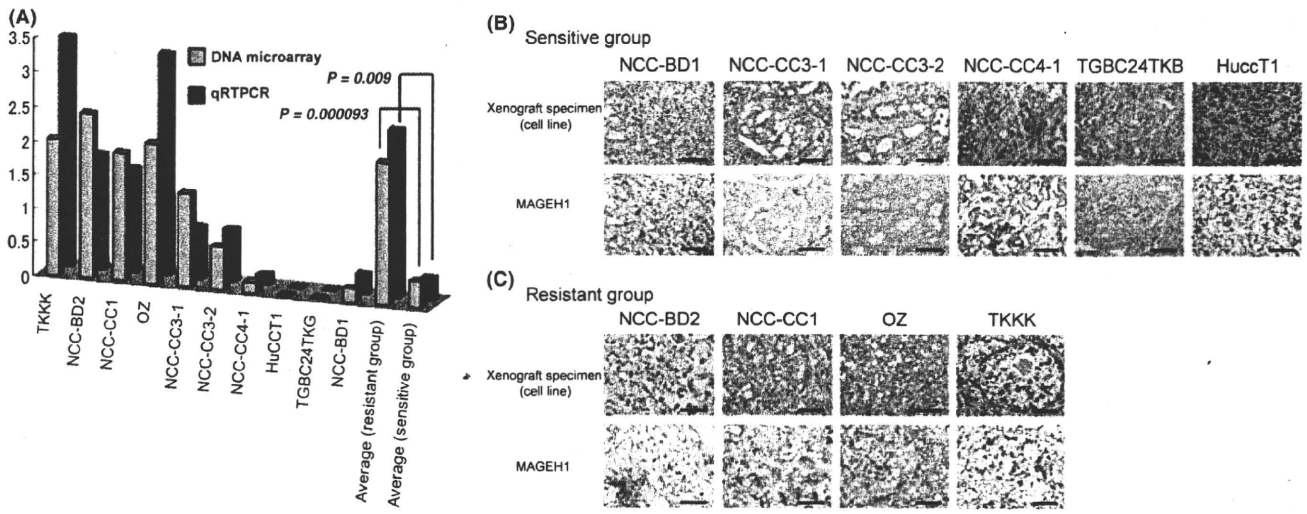

Fig. 3. (A) MAGEH1 mRNA expression in 10 biliary tract carcinoma cell lines. Relative expression of MAGEH1 mRNA compared to GAPDH expression in each cell line was quantified by microarray (blue columns) and quantitative RT-PCR (red columns). MAGEH1 expression was significantly different between gemcitabine (Gem)-sensitive and Gem-resistant groups. (B,C) Immunohistochemical analysis of MAGEH1 protein in xenograft specimens of 10 biliary tract carcinoma cell lines. Tumor histology (H&E staining) of xenograft specimens of cell lines, split into Gem-sensitive (B) and Gem-resistant (C) groups, and MAGEH1 protein expression detected by anti-MAGEH1 antibody in the same area are shown. All three cell lines that lacked MAGEH1 expression belong to the Gem-sensitive group. Scale line = 200 μm.

all four cell lines (100%) in the resistant group were positive for MAGEH1 expression (Fig. 3).

We selected nine recurrent BTC cases treated with gemcitabine alone, which were fully evaluated for drug effects by imaging diagnosis, as described in the "Materials and Methods" section, and whose tumor samples had been sufficiently examined and pathologically diagnosed. After clinical evaluation, we identified five "effective" cases and four "non-effective" cases (Table S2). We examined MAGEH1 protein expression in surgical specimens of the primary tumor in these nine cases. As shown in Figure 4, two (40%) of five "effective" cases were positive, and all four "non-effective" cases (100%) were positive.

Discussion

Elucidation of the molecular mechanisms determining the biological characteristics of cancer cells is one strategy for improving the clinical outcome of BTC patients, but only a few BTC cell lines serving as potent biological tools and animal models with properties resembling those of human cancer have been established. In this study, we succeeded in establishing six novel BTC cell lines including various subtypes and 19 BTC xenograft models after trying 55 cases. Despite carrying out multiple transplantations, we did not observe any marked discrepancy in cell morphology between the original tumors and the cell lines/xenografts, suggesting that this model could be stable and useful for biological studies. Moreover, we were able to fully combine the corresponding clinical information for patients and pathological archive specimens of primary tumors and xenografts for both primary tumors and cell lines with biological data on the cell lines for both basic and preclinical research. To add more clinically relevant functional data, we examined the gemcitabine sensitivities of these cell lines.

Previously, several predictive markers for the effects of gemcitabine chemotherapy have been reported in various types of tumor, including equilibrative nucleoside transporter-1 (hENT1),[10] ribonucleotide reductase subunit M2 (RRM2),[11] and heat shock protein 27 (HSP27)[12] for pancreatic carcinoma, ribonucleotide reductase subunit M1 (RRM1)[13] for non-small-cell lung cancer (NSCLC), hENT1 for ampulla of Vater carcinoma,[14] carcinoembryonic antigen-related cell adhesion

doi: 10.1111/j.1349-7006.2009.01462.x

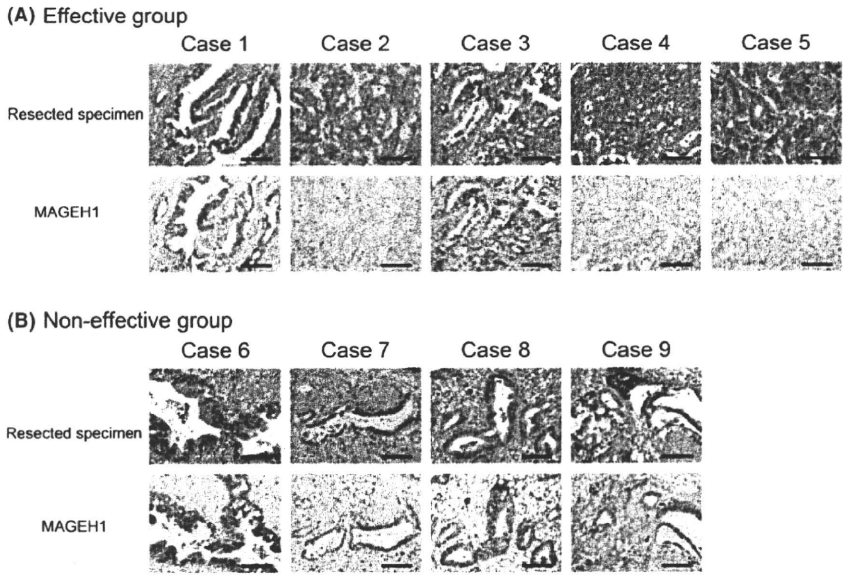

Fig. 4. Immunohistochemical analysis of MAGEH1 protein in primary tumor specimens of gemcitabine (Gem)-effective and non-effective groups. Tumor histology (H&E staining) of primary tumor specimens, split into Gem-effective (A) and Gem-non-effective (B) groups and MAGEH1 protein expression detected by anti-MAGEH1 antibody in the same area are shown. All three cases that lacked MAGEH1 expression belong to the Gem-effective group. Scale line = 200 μm.

molecule 6 (CEACAM6) for intrahepatic cholangiocarcinoma,[5] and RRM1 for biliary tract carcinoma.[15] Among these previously reported biomarkers, our microarray analysis validated that RRM2 expression was significantly ($P = 0.03$) increased (three-fold on average) in the resistant group compared to the sensitive one (data not shown). However, most of these studies analyzed a small number of cell lines (maximum two), for example, comparing a gemcitabine-sensitive cancer cell line with its subclone that had acquired gemcitabine resistance, and focused on molecules that are already known to be associated with gemcitabine transport and metabolism. No study has yet tested its efficacy in clinical samples. The present study examined the largest number of BTC cell lines to be detailed in published reports to date, including six novel ones, in relation to clinicopathological information. To discover potential biomarkers in an unbiased way, we examined genome-wide expression profiles using a microarray, identified several biomarker candidates including MAGEH1, and validated its significance in another cohort of clinical BTC cases.

MAGEH1 is a member of the melanoma antigen family (MAGE)[16]. The human MAGE family was originally identified as a tumor-specific antigen,[17] and is now classified into two subtypes (type I and type II).[18] Type I MAGE is completely silenced in normal tissues except male germ cells and placenta, whereas type II MAGE is expressed in both tumors and a fraction of normal tissues. MAGEH1 belongs to the type II MAGE family and is also expressed in normal human tissues.[16] MAGEH1 is expressed in 69% of NSCLC[19] and in 100% of renal cell carcinomas,[20] but no data for BTC have been reported. MAGEH1 associates with the intracellular domain of the p75/NGF receptor[21] and regulates the cell cycle,[19] but its precise role in cancer is largely unknown. In the Gene Expression Omnibus (GEO) database at National Center for Biotechnology Information (NCBI) (http://www.ncbi.nlm.nih.gov/geo/), there is one set of public microarray data showing the association between MAGEH1 expression and gemcitabine resistance in NSCLC cells. Comparison of the gene expression profile of parental Calu3 cell with those of gemcitabine-resistant subclones (Calu3-GemR) revealed that the mean expression of MAGEH1 mRNA in Calu3-GemR clones was more than twice as high as that in the parental cells.[22] However, there was no significant difference between the two, probably because of the small sample size analyzed ($P = 0.2481$; Fig. S1).

We further investigated whether MAGEH1 protein expression can be used for predicting clinical response to gemcitabine treatment, as protein expression is more stable and easier to test in clinical samples than RNA expression. Consistent with the mRNA expression data, we found that MAGEH1 protein was expressed in all resistant and non-effective cases. However, MAGEH1-positive cases also included a portion of sensitive or effective cases, possibly because of post-translational regulation of MAGEH1 protein expression. Significantly, however, MAGEH1-negative cell lines and primary cases were all gemcitabine-sensitive or effective cases, suggesting that MAGEH1 expression could be used as a negative predictor of gemcitabine response. That is, if immunohistochemical staining for MAGEH1 is negative, it is highly likely that a particular case would respond to gemcitabine therapy. Based on its previously reported functions, it remains unclear why MAGEH1 expression would be inversely correlated with gemcitabine response. It could function as a regulator of gemcitabine metabolism or might simply be a surrogate marker of distinct BTC subtypes. Because we analyzed only cases for which the result of gemcitabine treatment had been assessed objectively, it was difficult to collect a large number of retrospective cases. Moreover, we were unable to examine the expression of MAGEH1 RNA in the clinical specimens by RT-PCR because only small amounts of the frozen samples were available. Therefore, further prospective analysis of a larger cohort will be necessary to determine the clinical efficacy of MAGEH1 expression as a predictive biomarker of gemcitabine response.

Recently, a report has indicated that both the amount of stroma and vascularity in the tumor are associated with gemcitabine sensitivity in pancreatic cancer.[23] It was proposed that the hypovascularity and poor vascular architecture of pancreatic ductal carcinomas might impose an additional limitation to therapeutic delivery. Therefore, it was hypothesized that disrupting the stroma of pancreatic tumors might alter the vascular network

and thereby facilitate the delivery of chemotherapeutic agents. Accordingly, we recognized that the tumors in the non-effective group showed a tendency to have more of the stromal component than the tumors in the effective group (Fig. 4). Thus the stromal component would also play an important role in drug resistance of BTC.

In spite of the limited number of cases we examined, our result is consistent with the idea that more complex mechanisms regulate the gemcitabine sensitivity of BTC. In this sense, combination of other biomarker candidates obtained from the present screening or ones discovered through different approaches such as proteomic analysis with MAGEH1 should predict the drug response more accurately. In any event, the present study has shown that our new resource with clinical annotation would be valuable for discovering new biomarkers, and future studies for identifying new therapeutic/diagnostic targets are warranted.

Acknowledgments

This work was supported by a Grant-in-Aid for Cancer Research from the Ministry of Health, Labor and Welfare of Japan, a Grant-in-Aid for the Third Term Comprehensive 10-Year Strategy for Cancer Control from the Ministry of Health, Labor and Welfare of Japan, and a grant from the program for Promotion of Fundamental Studies in Health Sciences of the National Institute of Biomedical Innovation.

References

1 Washburn WK, Lewis WD, Jenkins RL. Aggressive surgical resection for cholangiocarcinoma. *Arch Surg* 1995; **130**: 270–6.
2 Kosuge T, Yamamoto J, Shimada K, Yamasaki S, Makuuchi M. Improved surgical results for hilar cholangiocarcinoma with procedures including major hepatic resection. *Ann Surg* 1999; **230**: 663–71.
3 Jang JY, Kim SW, Park DJ *et al.* Actual long-term outcome of extrahepatic bile duct cancer after surgical resection. *Ann Surg* 2005; **241**: 77–84.
4 Sakamoto Y, Kosuge T, Shimada K *et al.* Prognostic factors of surgical resection in middle and distal bile duct cancer: an analysis of 55 patients concerning the significance of ductal and radial margins. *Surgery* 2005; **137**: 396–402.
5 Ieta K, Tanaka F, Utsunomiya T, Kuwano H, Mori M. CEACAM6 gene expression in intrahepatic cholangiocarcinoma. *Br J Cancer* 2006; **95**: 532–40.
6 Khan SA, Thomas HC, Davidson BR, Taylor Robinson SD. Cholangiocarcinoma. *Lancet* 2005; **366**: 1303–14.
7 Thongprasert S. The role of chemotherapy in cholangiocarcinoma. *Ann Oncol* 2005; **16** (Suppl 2): ii93–6.
8 Shi X, Liu S, Kleeff J, Friess H, Buchler MW. Acquired resistance of pancreatic cancer cells towards 5-Fluorouracil and gemcitabine is associated with altered expression of apoptosis-regulating genes. *Oncology* 2002; **62**: 354–62.
9 Eisenhauer EA, Therasse P, Bogaerts J *et al.* New response evaluation criteria in solid tumours: revised RECIST guideline (version 1.1). *Eur J Cancer* 2009; **45**: 228–47.
10 Nakano Y, Tanno S, Koizumi K *et al.* Gemcitabine chemoresistance and molecular markers associated with gemcitabine transport and metabolism in human pancreatic cancer cells. *Br J Cancer* 2007; **96**: 457–63.
11 Duxbury MS, Ito H, Zinner MJ, Ashley SW, Whang EE. RNA interference targeting the M2 subunit of ribonucleotide reductase enhances pancreatic adenocarcinoma chemosensitivity to gemcitabine. *Oncogene* 2004; **23**: 1539–48.
12 Mori Iwamoto S, Kuramitsu Y, Ryozawa S *et al.* Proteomics finding heat shock protein 27 as a biomarker for resistance of pancreatic cancer cells to gemcitabine. *Int J Oncol* 2007; **31**: 1345–50.
13 Rosell R, Danenberg KD, Alberola V *et al.* Ribonucleotide reductase messenger RNA expression and survival in gemcitabine/cisplatin-treated advanced non-small cell lung cancer patients. *Clin Cancer Res* 2004; **10**: 1318–25.
14 Santini D, Perrone G, Vincenzi B *et al.* Human equilibrative nucleoside transporter 1 (hENT1) protein is associated with short survival in resected ampullary cancer. *Ann Oncol* 2008; **19**: 724–8.
15 Ohtaka K, Kohya N, Sato K *et al.* Ribonucleotide reductase subunit M1 is a possible chemoresistance marker to gemcitabine in biliary tract carcinoma. *Oncol Rep* 2008; **20**: 279–86.
16 Chomez P, De Backer O, Bertrand M, De Plaen E, Boon T, Lucas S. An overview of the MAGE gene family with the identification of all human members of the family. *Cancer Res* 2001; **61**: 5544–51.
17 van der Bruggen P, Traversari C, Chomez P *et al.* A gene encoding an antigen recognized by cytolytic T lymphocytes on a human melanoma. *Science* 1991; **254**: 1643–7.
18 Barker PA, Salehi A. The MAGE proteins: emerging roles in cell cycle progression, apoptosis, and neurogenetic disease. *J Neurosci Res* 2002; **67**: 705–12.
19 Tsai JR, Chong IW, Chen YH *et al.* Differential expression profile of MAGE family in non-small-cell lung cancer. *Lung Cancer* 2007; **56**: 185–92.
20 Kramer BF, Schoor O, Kruger T *et al.* MAGED4-expression in renal cell carcinoma and identification of an HLA-A*25-restricted MHC class I ligand from solid tumor tissue. *Cancer Biol Ther* 2005; **4**: 943–8.
21 Tcherpakov M, Bronfman FC, Conticello SG *et al.* The p75 neurotrophin receptor interacts with multiple MAGE proteins. *J Biol Chem* 2002; **277**: 49101–4.
22 Tooker P, Yen WC, Ng SC *et al.* Bexarotene (LGD1069, Targretin), a selective retinoid X receptor agonist, prevents and reverses gemcitabine resistance in NSCLC cells by modulating gene amplification. *Cancer Res* 2007; **67**: 4425–33.
23 Olive KP, Jacobetz MA, Davidson CJ *et al.* Inhibition of Hedgehog signaling enhances delivery of chemotherapy in a mouse model of pancreatic cancer. *Science* 2009; **324**: 1457–61.

Supporting Information

Additional Supporting Information may be found in the online version of this article:

Fig. S1. Mircoarray data of association between MAGEH1 and gemcitabine in non-small lung cancer from NCBI GEO database.

Table S1. Primers for mutation analysis of *p53* and *KRAS* genes.

Table S2. Clinicopathological feature of 9 patients.

Please note: Wiley-Blackwell are not responsible for the content or functionality of any supporting materials supplied by the authors. Any queries (other than missing material) should be directed to the corresponding author for the article.

doi: 10.1111/j.1349-7006.2009.01462.x

J Gastrointest Surg (2010) 14:335–343
DOI 10.1007/s11605-009-1072-7

ORIGINAL ARTICLE

Surgical Management of Infrahilar/Suprapancreatic Cholangiocarcinoma: an Analysis of the Surgical Procedures, Surgical Margins, and Survivals of 77 Patients

Yoshihiro Sakamoto · Kazuaki Shimada · Satoshi Nara · Minoru Esaki · Hidenori Ojima · Tsuyoshi Sano · Junji Yamamoto · Tomoo Kosuge

Received: 18 June 2009 / Accepted: 16 October 2009 / Published online: 10 November 2009

Abstract
Background Optical surgical management of infrahilar/suprapancreatic cholangiocarcinoma remains controversial.
Methods Between 1988 and 2006, 77 patients with infrahilar/suprapancreatic cholangiocarcinoma underwent curative surgical resections following our intention-to-treat strategy. The clinicopathological factors affecting survival were evaluated using univariate and multivariate analyses with regard to the surgical procedures and surgical margins.
Results The surgical procedure included extrahepatic bile duct resection alone (EHBD; $n=17$), major hepatectomy combined with extrahepatic bile duct resection (MHx; $n=26$), pancreaticoduodenectomy (PD; $n=28$), and MHx and concomitant PD (HPD; $n=6$). Performance of MHx and/or PD in addition to EHBD increased surgical morbidity ($p=0.001$). Among patients undergoing the four surgical procedures (EHBD, MHx, PD, and HPD), no significant difference was found in the incidence of positive overall surgical margins (53%, 65%, 46%, and 67%, $p=0.51$) or long-term survivals (median survival time, 51, 27, 41, and 22 months, $p=0.60$). A multivariate analysis revealed that perineural invasion (95% confidence interval, 1.1–12.3, $p=0.009$), nodal metastasis (1.6–6.8, $p=0.001$), and blood transfusion (1.1–3.9, $p=0.02$) were independent predictors of a poor outcome. Perineural invasion was associated with positive radial margins ($p=0.045$) and submucosal ductal infiltration ($p=0.03$).
Conclusion Perineural invasion, rather than the type of surgical procedure, had a significant impact on surgical curability and survival of patients with infrahilar/suprapancreatic cholangiocarcinoma treated according to our intention-to-treat strategy.

Keywords Cholangiocarcinoma · Upper and middle · Perineural invasion · Major hepatectomy · Pancreaticoduodenectomy

Y. Sakamoto (✉) · K. Shimada · S. Nara · M. Esaki · T. Kosuge
Hepatobiliary and Pancreatic Surgery Division,
National Cancer Center Hospital,
5-1-1 Tsukiji, Chuo-ku, Tokyo 104-0045, Japan
e-mail: yosakamo@ncc.go.jp

H. Ojima
Pathology Division, National Cancer Center Research Institute,
Tokyo, Japan

T. Sano
Department of Gastroenterological Surgery,
Aichi Cancer Center Hospital,
Nagoya, Japan

J. Yamamoto
Department of Surgery, National Defense Medical College,
Tokyo, Japan

Introduction

Recent advances in imaging modalities and surgical strategies have improved the outcome of the surgical treatment for cholangiocarcinoma. Surgical resection for perihilar cholangiocarcinoma often involves major hepatectomy combined with extrahepatic bile duct resection (MHx) following preoperative biliary drainage and portal vein embolization.[1–7] In highly select institutions, the mortality of MHx for perihilar cholangiocarcinoma has been reduced to less than 1%,[3–5,7] and the 5-year survival rate has been increased up to 40%.[4,7] Pancreaticoduodenectomy (PD) has long been a standard procedure for middle or distal cholangiocarcinoma. The reported 5-year survival rate is 24–39%, and the surgical mortality is reported to be 2–7%.[8–15]

However, surgical treatment for infrahilar/suprapancreatic cholangiocarcinoma has never been fully discussed. Infrahilar/suprapancreatic bile duct can be classified into the superior or middle bile ducts according to the Japanese classification.[16]

Superior cholangiocarcinoma corresponds to Bismuth types I and II cholangiocarcinoma,[17] and middle cholangiocarcinoma corresponds to classical middle third cholangiocarcinoma.[18,19] These types of cholangiocarcinoma are originated from the bile duct in the hepatoduodenal ligament and not only do they often involve the adjacent hepatic artery and portal vein but they also often extend along the biliary tract in a mucosal and/or submucosal fashion.[20] Therefore, extrahepatic bile duct resection (EHBD) is sometimes insufficient to secure negative surgical margins and MHx and/or PD in addition to EHBD is required to obtain a favorable prognosis.[21,22] MHx with concomitant PD (HPD) enables the extensive resection of biliary trees, but it is associated with significantly higher morbidity and mortality rates. Consequently, surgical procedure for the removal of infrahilar/suprapancreatic cholangiocarcinoma should be determined on the balance of the surgical curability and safety. In this study, we reviewed the medical records of 77 patients undergoing curative surgical resection with pathologically proven infrahilar/suprapancreatic cholangiocarcinoma and determined the prognostic factors for survival with regard to the impact of surgical procedures and surgical margins.

Patients and Methods

Between 1988 and 2006, 212 patients with extrahepatic cholangiocarcinoma underwent resectional surgery in the Hepatobiliary and Pancreatic Surgery Division, National Cancer Center Hospital, Tokyo. They were classified into hilar (n=92), superior or middle (n=77), and distal (n=43) cholangiocarcinoma, as determined using the final pathological diagnosis according to the Japanese classification as follows[16]: hilar, arising from the hilar bile duct; superior or middle, arising from the infrahilar/suprapancreatic bile duct; and distal, arising from the intrapancreatic bile duct. The infrahilar/suprapancreatic bile duct was equally divided into two parts; the upper part was termed as the "superior" bile duct, and the lower part was termed the "middle" bile duct.[16] In the present study, clinicopathological data on patients with superior or middle cholangiocarcinoma was reviewed.

Indication of Surgical Procedures

Preoperatively, the predominant location of the tumor and the extent of the tumor along the biliary tract were evaluated using imaging studies, including an enhanced computed tomography scan, ultrasonography, magnetic resonance imaging, cholangiography, and angiography. The surgical procedure was decided by each attending surgeon after considering the balance between the tumor extent and the safety of each surgical procedure, following our intention-to-treat strategy. All patients with obstructive jaundice underwent preoperative biliary drainage with a percutaneous approach via the future remnant hemiliver, in principle.[3,4,7] MHx and PD were performed after the serum total bilirubin concentrations had decreased to less than 2 and 5 mg/dL, respectively.

After laparotomy and the exclusion of distant metastasis, all of the following four surgical procedures included a regional lymphadenectomy at the hepatoduodenal ligament, the upper part of the retropancreatic area, and the common hepatic artery. In patients with localized cholangiocarcinoma in the hepatoduodenal ligament, EHBD with lymphadenectomy was adopted, especially in patients with a poor general condition or high-risk factors.

When the tumor was predominantly located in the superior bile duct or tumor involvement in the right hepatic artery was observed on the preoperative images, an extended right hemihepatectomy combined with EHBD was scheduled, following preoperative portal embolization of the right hemiliver. The caudate lobe was completely removed during extended right hemihepatectomy. When the tumor was predominantly located in the left hemiliver, an extended left hemihepatectomy with EHBD was performed without preoperative portal vein embolization. The Spiegel lobe and part of the paracaval portion of the caudate lobe were removed, but part of the caudate process was sometimes preserved during extended left hemihepatectomy. The indications for preoperative portal vein embolization and the fundamental strategy for major hepatectomy are described elsewhere.[1,3,4,7]

When the tumor was predominantly located in the middle and distal bile duct, PD was performed.[15] Since 2000, pylorus-preserving PD (PPPD) has become the standard procedure, rather than the standard Whipple procedure.

HPD was indicated in patients with widespread cholangiocarcinoma or in patients with infrahilar/suprapancreatic cholangiocarcinoma involving the right hepatic artery, when the general condition of the patient was favorable. Preoperative portal embolization was performed in all the patients undergoing HPD.

When the tumor involved the major portal vein, aggressive combined resection of the portal vein and reconstruction was performed. When the tumor involved the future remnant main hepatic artery, hepatic arterial resection and reconstruction was performed under a surgical microscope by plastic surgeons.[23]

Diagnosis and Definition of Surgical Margins

Intraoperative evaluation of the hepatic-side and/or duodenal-side ductal margins was performed using frozen sections in all patients. When the duodenal-side ductal margin was positive, additional resection of the intrapancreatic bile duct was performed, as far as possible and in principle. When the hepatic-side ductal margin was positive, additional resection of the hepatic duct was performed, if possible. Positive surgical margins were classified into two categories: "mucosal

infiltration" and "submucosal infiltration".[20] When the ductal margins were positive for both mucosal and submucosal infiltration, they were defined as positive for submucosal infiltration in the following discussion: Radial margins were defined as surgical margins other than the ductal margins of the resected specimen.

Definition of Surgical Complications

Postoperative pancreatic fistula was defined according to the definition proposed by an international study group on pancreatic fistula[24]: an amylase concentration in the drain fluid (obtained on or after postoperative 3) greater than three times the standard serum amylase concentration. Pancreatic fistulas were classified into grades A, B, or C according to severity: briefly, grade A, a "transient fistula" that was not associated with a delay in hospital discharge; grade B, a fistula that led to a delay in discharge, with persistent drainage for more than 3 weeks; and grade C, a fistula that was usually associated with major complications. Grades B and C fistulas were considered significant complications. Delayed gastric emptying (DGE) was classified into grades A, B, and C according to the definitions used in the recently report[25]: grade A, unable to tolerate solid oral intake by postoperative day 7 but vomiting is uncommon; grade B, unable to tolerate solid oral intake by postoperative day 14 and vomiting is common; and grade C, unable to tolerate solid oral intake by postoperative day 21 and vomiting is common. Grades B and C DGE were considered significant complications. Postoperative hepatic insufficiency was defined as an increase in the postoperative total bilirubin value of more than 10 mg/dL.

Comparison of Clinicopathological Variables Among the Four Procedures

The clinicopathological variables were compared among the four groups of patients undergoing each procedure: EHBD, MHx, PD, and HPD. All of the sequential parameters were dichotomized at the median value of each variable.

Univariate and Multivariate Analyses of the Predictors of Survival

A univariate analysis of the two groups was performed using the following categorized variables: age (≥65, <65 years), gender, period of surgical resection (1988–2000 vs. 2001–2006), surgical procedures (EHBD, MHx, PD, HPD), operative time (≥10, <10 h), blood loss (≥1,200, <1,200 mL), blood transfusion, morbidity, dominant location of the tumor (superior vs. middle bile duct), tumor differentiation (papillary to well-differentiated adenocarcinoma vs. moderately to poorly differentiated adenocarcinoma), depth of tumor infiltration (T1 vs. T2 or T3 in TNM classification[26]), presence or absence of pathological lymphatic invasion, venous invasion, perineural invasion, nodal metastasis (N factor in TNM classification[26]), distant metastasis (M factor in TNM classification[26] including hepatic metastasis and para-aortic nodal metastasis), status of hepatic-side ductal margin, duodenal-side ductal margin, overall ductal margins, radial margin, and overall surgical margins. Each threshold value was determined according to the median value of each category. A multivariate analysis was performed using factors that proved to be significant in the univariate analysis.

Statistical Analysis

The results are reported as the median and range unless otherwise specified. A parametric statistical analysis was performed using the chi-square analysis or Fisher's exact test. The cumulative survival rates were generated using the Kaplan–Meier method; and the difference between the rates of the groups was assessed using the log-rank test. Statistical significance was defined as a p value of less than 0.05. The statistical analyses were performed using a statistical analysis software package (SPSSII 11.0, SPSS Inc., Chicago, IL, USA).

Results

Summary of Surgical Procedures

The surgical procedures for infrahilar/suprapancreatic cholangiocarcinoma included EHBD alone (n=17), MHx combined with EHBD (n=26), PD (n=28), and MHx and concomitant PD (n=6). The hepatectomy procedures consisted of extended right hemihepatectomy (n=19), right trisegmentectomy (n=1), extended left hemihepatectomy (n=5), left trisegmentectomy (n=1), and right HPD (n=6). The PD procedures consisted of PPPD (n=18) and the standard Whipple procedure (n=10). Combined portal vein resection was performed in 12 patients (16%), and hepatic artery resection and reconstruction was performed in two patients (3%).

Overall surgical morbidity was 71%, and two patients (2.6%) died as a result of surgery; one patient who underwent an extended left hemihepatectomy plus EHBD died of intra-abdominal bleeding and hepatic insufficiency on day 6, and another patient who underwent EHBD died of intra-abdominal bleeding on day 8. No deaths occurred after 1999. The overall 5-year survival arte and median survival time of the 77 patients were 32% and 38 months, respectively.

Comparison of the Four Surgical Procedures

Table 1 showed the comparative results among the four surgical procedures. Selection of the surgical procedure was

Table 1 Comparison of Clinicopathological Variables Among the Four Groups of Patients Undergoing Four Types of Surgical Procedures in the Management of Superior or Middle Cholangiocarcinoma

		EHBD (n=17)	MHx (n=26)	PD (n=28)	HPD (n=6)	p value
Surgical period	1988–2000	11	10	8	1	0.06
	2001–2006	6	16	20	5	
Age (year)	<65	5	11	12	3	0.76
	≥65	12	15	16	3	
Predominant location	Bs	6	18	3	3	<0.001*
	Bm	11	8	25	3	
Operative time (min)	<600	14	11	16	0	0.003*
	≥600	3	14	12	6	
Blood loss (mL)	<1,200	15	8	16	0	<0.001*
	≥1,200	2	18	12	6	
Additional ductal resection	Performed (%)	9 (53%)	13 (50%)	12 (43%)	4 (67%)	0.73
Blood transfusion	Performed	2 (12%)	7 (27%)	9 (32%)	3 (50%)	0.27
Morbidity	Overall	6 (35%)	19 (73%)	24 (86%)	6 (100%)	0.001*
	POPF	2 (12%)	4 (15%)	22 (79%)	5 (83%)	<0.001*
	Bile leakage	1 (6%)	12 (46%)	3 (11%)	2 (33%)	0.004*
	DGE	6 (35%)	4 (15%)	13 (46%)	4 (67%)	0.035*
	Cholangitis	2 (12%)	5 (19%)	3 (11%)	1 (17%)	0.84
	Hepatic failure	0	0	0	1 (17%)	0.007*
Hospital stay (days)	<35	11	12	10	2	0.26
	≥35	6	14	18	4	
Mortality		1 (6%)	1 (4%)	0	0	0.62
T factor	T1	4	1	1	1	0.09
	T2–4	13	25	27	5	
Nodal status	Positive	7 (41%)	18 (69%)	14 (50%)	5 (83%)	0.13
M factor	M1	0	4 (15%)	1 (4%)	0	0.15
Perineural invasion	Positive	12 (71%)	22 (85%)	25 (89%)	6 (100%)	0.25
Clinical stage	I, II	17	21	26	6	0.13
	III, IV	0	5	2	0	
Overall surgical margin	Positive	9 (53%)	17 (65%)	13 (46%)	4 (67%)	0.51
Hepatic-side ductal margin	Positive	8 (47%)	11(42%)	10 (36%)	2 (33%)	0.87
	Mucosal	4	5	6	1	
	Submucosal	4	6	4	1	
Duodenal-side ductal margin	Positive	5 (29%)	14 (54%)	0	0	<0.001*
	Mucosal	3	8	0	0	
	Submucosal	2	6	0	0	
Radial margin	Positive	6 (35%)	3 (8%)	6 (21%)	2 (33%)	0.28

Three M1 patients in hepatectomy group were found to have hepatic metastasis, and the remaining two M1 patients had para-aortic nodal metastasis

EHBD extrahepatic bile duct resection, *MHx* major hepatectomy, *PD* pancreaticoduodenectomy, *HPD* major hepatectomy plus pancreaticoduodenectomy, *Bs* superior bile duct, *Bm* middle bile duct, *POPF* postoperative pancreatic fistula (grade B or C), *DGE* delayed gastric emptying (grade B or C)

related to the predominant location of the tumor. Performance of MHx and/or PD in addition to EHBD was associated with increased operative time, blood loss, and surgical morbidities, but not with the hospital stay and mortality. PD guaranteed negative duodenal-side ductal margin; however, the incidence of positive overall surgical margin was comparable among the four groups of patients undergoing four types of surgical procedures.

Univariate and Multivariate Analyses of Prognostic Factors

In the univariate analysis of prognostic variables, blood transfusion, depth of tumor invasion (T2, T3), nodal metastasis, distant metastasis, perineural invasion, and a positive radial margin were significantly predictors of a poor outcome (Table 2). A multivariate analysis of these six variables revealed that blood transfusion, nodal metastasis,

Table 2 Univariate Analysis of Prognostic Factors of 77 Patients Undergoing Surgical Resection for Superior or Middle Cholangiocarcinoma

		Number	Overall 5-year survival rate (%)	MST (months)	*p* value
Patient characteristics					
Age	≤65	35	41	51	0.21
	>65	42	24	34	
Gender	Male	57	36	38	0.25
	Female	20	23	29	
Operative period	1988–2000	30	30	38	0.85
	2001–2006	47	37	33	
Surgical parameters					
Surgical procedure	EHBD	17	29	51	0.60
	MHx	26	32	27	
	PD	28	35	41	
	HPD	6	44	22	
Operative time	<10 h	41	32	51	0.18
	≥10 h	35	38	33	
Blood loss	<1,200 mL	39	30	51	0.29
	≥1,200 mL	38	38	29	
Blood transfusion	Not performed	56	36	51	0.02*
	Performed	21	21	24	
Morbidity	Absent	22	29	51	0.37
	Present	55	33	34	
Pathological factors					
Dominant location	Bs	30	30	28	0.36
	Bm	47	35	51	
Differentiation[a]	pap, well	29	32	51	0.24
	mod, por	47	34	33	
T factor in TNM	T1	7	100	ND	0.01*
	T2, T3	70	27	33	
Lymphatic invasion	Absent	11	60	83	0.054
	Present	66	28	33	
Venous invasion	Absent	20	53	75	0.15
	Present	57	24	33	
Perineural invasion	Absent	12	132	69	0.005*
	Present	65	23	33	
N factor in TNM	N0	33	52	75	0.0004*
	N1	44	16	26	
M factor in TNM	M0	72	33	36	0.048*
	M1	5	ND	15	
Hepatic-side ductal margin	Negative	46	34	33	0.98
	Positive	31	24	39	
Duodenal-side ductal margin	Negative	58	31	33	0.58
	Positive	19	34	51	
Overall ductal margins	Negative	41	30	33	0.52
	Positive	36	35	51	
Radial margin	Negative	60	38	51	0.03*
	Positive	17	10	23	
Overall surgical margin	Negative	34	35	38	0.47
	Positive	43	29	39	

T and N factors are determined by TNM classification of malignant tumors, 6th edition

EHBD extrahepatic bile duct resection, *MHx* major hepatectomy, *PD* pancreaticoduodenectomy, *HPD* major hepatectomy plus pancreaticoduodenectomy, *Bs* superior bile duct, *Bm* middle bile duct, *pap* papillary adenocarcinoma, *well* well-differentiated adenocarcinoma, *mod* moderately differentiated adenocarcinoma, *por* poorly differentiated adenocarcinoma

*$p<0.05$

[a] Excluding one patient with mucinous carcinoma

and perineural invasion were independent predictors of a poor outcome (Table 3). No significant survival difference was found among the four groups of patients undergoing the four procedures (Fig. 1).

Perineural invasion was positive in all the patients with a positive radial margin (n=17) or a positive intestinal ductal margin (n=19). There was a significant relationship between perineural invasion and a positive radial margin (p=0.045) and between perineural invasion and a positive submucosal ductal margin (p=0.03; Table 4).

Ductal Margin Status and Local Recurrence

The frozen section was positive in 32 patients, but it turned to be negative on the permanent section in one patient. The positive predictive value was 0.97. The frozen section was negative in 45 patients, but it turned to be positive on the frozen section in five patients. Thus, the negative predictive value was 0.89. Among the 36 patients with a positive ductal margin, 17 patients had only mucosal infiltration, while 19 patients had submucosal infiltration. One of the 17 patients with positive mucosal infiltration (6%) developed a ductal recurrence, while eight of the 19 patients with positive submucosal infiltration developed a ductal recurrence (42%); the incidence of ductal recurrence was significantly higher in patients with submucosal infiltration than in patients with mucosal infiltration (p=0.01). Among the 31 patients with positive hepatic-side ductal margins, the survival of patients with positive submucosal infiltration (n=16) was worse than that of patients with only positive mucosal infiltration (n=15, p=0.004; Fig. 2).

Discussion

Although many authors have discussed the surgical treatment of perihilar and distal cholangiocarcinoma,[1–15] optical surgical management of infrahilar/suprapancreatic cholangiocarcinoma has not been discussed in a lump. As infrahilar/suprapancreatic cholangiocarcinoma is located midway of the biliary tree, four types of surgical procedures, i.e., EHBD, MHx, PD, and HPD, can be indicated for removal of the tumor. The present study clearly showed that the perineural invasion was significantly associated with incidence of positive radial and submucosal ductal margins and was also an independent predictive factor for survival together with blood transfusion and nodal metastasis. Performance of MHx and/or PD in addition to EHBD increased surgical morbidities, but the type of procedure did not have significant impact on the incidence of positive overall surgical margins or on the long-term survivals of patients, if applied according to our intention-to-treat strategy.

Table 3 Multivariate Analysis of Prognostic Factors of 77 Patients Undergoing Surgical Resection for Superior or Middle Cholangiocarcinoma

Variables	β	Risk ratio	95% CI	p value
Perineural invasion	1.433	4.191	1.428–12.295	0.009*
Nodal metastasis	1.210	3.354	1.644–6.843	0.001*
Blood transfusion	0.722	20.59	1.102–3.847	0.024*

*p<0.05

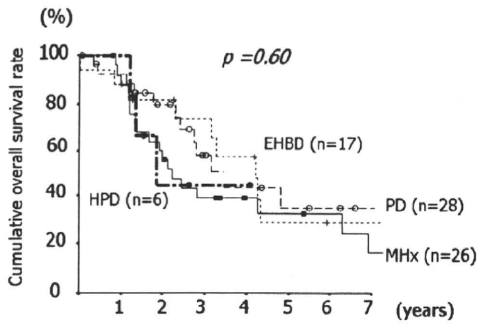

Figure 1 Cumulative overall survival of 77 patients with infrahilar/suprapancreatic cholangiocarcinoma treated with four types of surgical procedures. No significant difference was found in the survival of patients undergoing extrahepatic bile duct resection (*EHBD*; *dotted line with cross* (n=17)), major hepatectomy (*MHx*; *solid line with black square* (n=26)), pancreaticoduodenectomy (*PD*; *dotted line with white circle* (n=28)), or major hepatectomy plus pancreaticoduodenectomy (*HPD*; *bold line with black circle* (n=6); p=0.60).

Regarding the surgical treatment of perihilar cholangiocarcinoma, it has been repeatedly advocated that the surgical margin is an important prognostic factor.[1–4,6,9,11,13,14] In these reports, the ductal and radial margins were discussed together as the "surgical margin". We previously reported that when treating middle or distal cholangiocarcinoma, it is important to secure a negative radial margin, although it may be less beneficial to obtain a negative hepatic-side ductal margin.[15] In this study, the radial margin, which was associated with perineural invasion, was a predictor of survival according to a univariate analysis, but the ductal margin was not. Considering these results, when the radial margin is apparently positive, additional ductal resection for a positive ductal margin may not improve the survival of patients.

On the other hand, it is noteworthy that a positive submucosal ductal margin resulted in a higher incidence of local recurrence and a worse survival outcome, compared with the results for a positive mucosal ductal margin. The hepatic-side submucosal margin was a possible prognostic factor as shown in Fig. 2. As shown in Table 4, positive submucosal infiltration and positive ductal margins are strongly associated with perineural invasion, which proved to be an independent and significant prognostic factor. That is, the prognosis of patients might be largely influenced not by the ductal status but by the presence or absence of perineural